1.0 - INTRODUCTION

Within the last few decades, a large number of Unmanned Air Vehicles (UAVs) has been developed for use by the United States military. Currently, the only Unmanned Combat Air Vehicle (UCAV) in service is the General Atomics *Predator*, which has been modified to carry *Hellfire* missile. New-generation UCAV demonstrators are being produced by Boeing and Northrop Grumman, but these aircraft are designed for low mission endurance air-to-air and ground-attack roles. Incorporating the latest available technology, the Gisin Aviation *Molniya* combines the low-observable (LO) characteristics and the high loiter endurance required to achieve a balanced level of performance in the 2002-2003 AIAA Individual Aircraft Request for Proposal (RFP) medium-altitude surveillance/light attack mission.

1.1. Historical Background

Although most UAVs were originally built to perform a reconnaissance or target drone mission, many efforts to convert them to an attack role have taken place. In the 1972, the Teledyne Ryan *Firebee* RPV was tested launching both the AGM-65 *Maverick* and EO-guided bombs in simulated strikes against SAM sites. More recently, the General Atomics *Predator* was converted to carry two AGM-114 *Hellfire* missiles, and made history by repeated success in attacking targets in Afghanistan and Iraq. Although the *Predator/Hellfire* combination has proved itself to be an extremely valuable asset, a number of operational deficiencies are

Figure 1 – Firebee RPF

exhibited by the system. The *Predator* does not have stealth features, has a comparatively low cruise speed and has been shown to be vulnerable in poor weather conditions. It is also expensive to operate and support, requiring 5 times[1] the maintenance and support personnel than a comparable manned aircraft.

1.2. RFP Requirements

The 2002-2003 AIAA RFP stipulates a set of requirements for a vehicle to perform the Medium Altitude Long Endurance (MALE) UCAV mission and to act as a higher-technology and capability replacement for the *Predator* system. The main areas in which the RFP aircraft must supercede the *Predator* are: Higher survivability features, higher loiter time, an increase in cruise speeds and a longer range. The RFP specifies two mission profiles: a long-endurance Surveillance/Light Strike Mission and a shorter-endurance Quick Reaction Strike Mission. The profiles for both of the RFP missions can be seen in Figure 2.

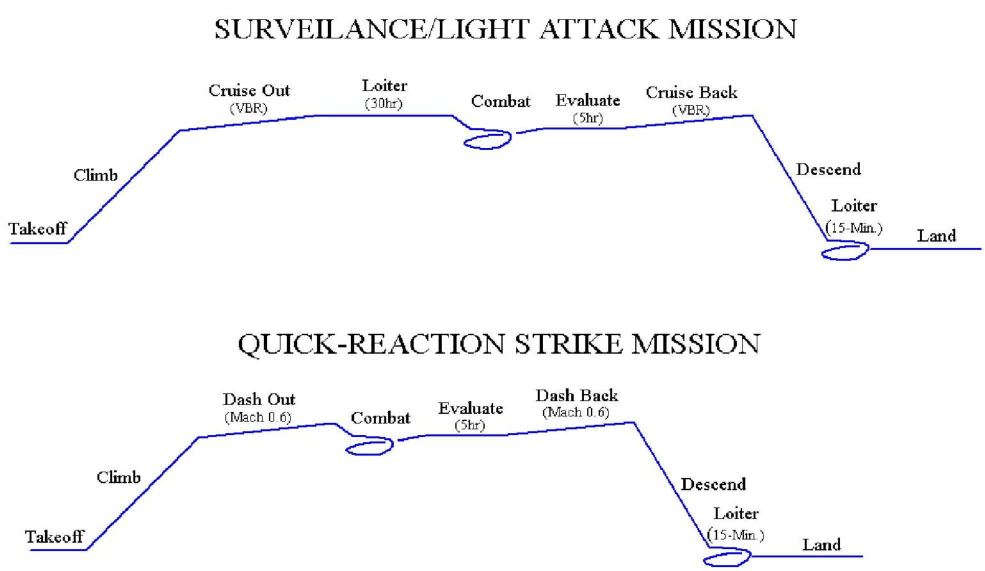

Figure 2 – *Molniya* Mission Profiles

1.3. Design Drivers

Upon detailed evaluation, a set of the RFP requirements revealed itself to be the design drivers in the design of the *Molniya*. The 5000-foot icy runway maximum rejected takeoff accelerate/stop distance was a requirement that drove both the installed thrust and the maximum CL of the wing. The tradeoff between LO characteristics and the efficiency required to enable a 35-hour loiter time was another trade that affected the aircraft sizing greatly. Finally, also as a factor of the extremely long loiter time the aircraft had to possess, the engine specific fuel consumption (SFC) was of great import. The extent to which *Molniya* adheres to the requirements of the RFP can be seen in the compliance matrix presented in **Table I**.

Table I - Molniya Compliance Matrix

RFP Requirement	*Molniya*	Compliance
System Cost < 20 Mil.	$M 14.2	✓
Balanced Observables	Reduced RCS, IR	✓
RTO = 5,000 ft	4,880 ft	✓
Dash at M=0.6	Dash at M=0.6	✓
1-g SEP = 100ft/s at 0.5M/25,000 ft	Exception Taken	
Max. 10% S. M.	CG @ 7.3% S.M.	✓

1.4. RFP Mission Evaluation

The RFP requirements are vague in some areas and required evaluation in order to define additional implied requirements. It was necessary to perform this evaluation early-on in the design process to ensure that the aircraft design progression would create a sound answer to the RFP and not stray.

The RFP mission's main focus is an aircraft which performs the mission of the Predator System, but with a higher capability in various performance regions. The tradeoff of LO and loiter endurance had to come to a solution which optimized the performance of the overall system. When some wing sweep trade studies were performed on a general aircraft configuration, it was obvious that with the moderate wing sweep required for low speed/long endurance loiter performance, an RCS level of the highly swept B-2 and F-22 aircraft could not be achieved in the forward quadrant (Figure 3).

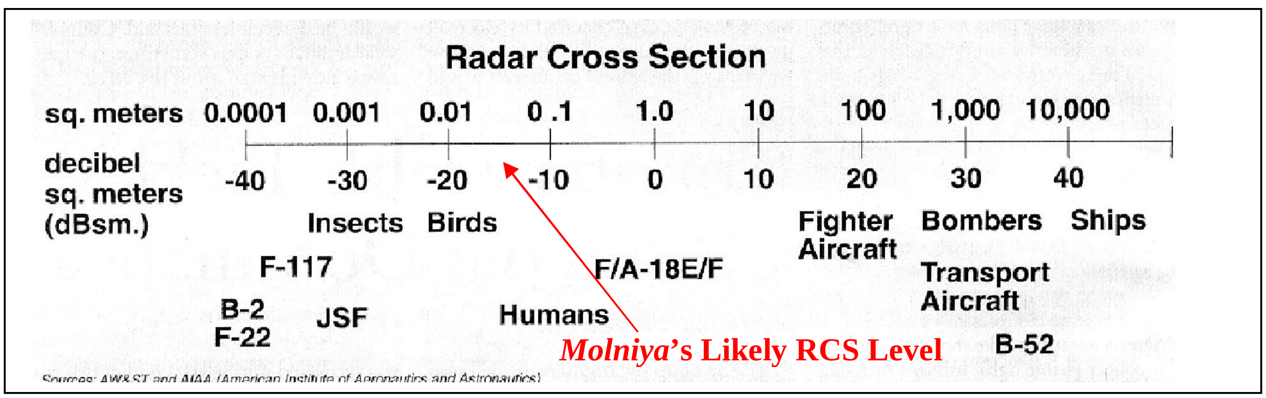

Figure 3 – Aircraft and RCS Scale (AW&ST and AIAA)

It was clear that *Molniya*'s design must not focus on direct penetration of enemy airspace and SEAD missions. Although this capability had to be developed to the highest extent possible, it was not to be the primary goal of the design. *Molniya* may be required to interdict targets of opportunity (such as SAM sites on the move), and report enemy movement to higher-capability attack-only UCAVs. With the –15 dBsm RCS that is obtainable for the configuration, *Molniya* will be able to operate unnoticed within the kill zone of many older SAM systems.

2.0 – CONCEPT EVALUATION

Having performed preliminary sizing for the mission requirements, a choice for the general configuration of the aircraft was deliberated upon. Some of the configuration types deliberated upon were the following: conventional, flying wing, twin boom and canard. With the initial concept selection being a very important step in an aircraft's design, it was crucial that the pros and cons of each configuration be evaluated. During initial concept selection, an emphasis was placed on finding an innovative configuration which could offer benefits not yet realized in mainstream aircraft design.

Conventional

The conventional configuration has a benefit of being a "safe bet", with little development needing to be done. However, this configuration is usually higher-drag than some other possible configurations because of the presence of a vertical and the negative lifting characteristic of the tail. This configuration generally suffers from having non-ideal stealth characteristics because of the right angles between the wing and the fuselage.

Flying Wing

The flying wing is extremely well suited for long-duration loitering flight. It is also a configuration that possesses a high degree of stealth by virtue of having little discontinuity in its geometry. Well-known problem of flying wings include aerodynamic flutter, low maximum C_L and landing gear integration issues. A sweptback untapered flying wing is a non-ideal planform which suffers from increased induced drag. Considering the high C_Ls of loitering flight, induced drag was an important factor to minimize. The low thrust-to-weight ratio of the aircraft necessitates either a large-area wing or a high-C_L airfoil in order to meet the takeoff constraint. The large-area wing, however, is a great disadvantage when flying the Mach 0.6 dash mission. With a cambered high-C_L airfoil appearing to be the optimum way to meet the takeoff constraint, a flying wing was at a distinct disadvantage because of its inability to trim out large coefficients of lift. Although possessing a number of potential disadvantages, the flying wing was decided to have enough merit to be investigated further.

Twin Boom

The twin boom configuration does not offer much benefit to the RFP mission. Traditionally, aircraft used twin booms to neatly fair motors and the main landing gear. Structural, low observability and increased drag issues result from this configuration.

Canard

The unstable canard configuration has a distinct set of advantages. First off, this configuration allows for L/D, because no lift is wasted by the reflexed airfoils and tails of the flying wing and conventional configurations, respectively. The canard aircraft would also be able to generate a high trimmed C_L on takeoff by the virtue of its high control authority. With an unstable configuration, the canard does not necessarily have to be designed to stall before the main wing, allowing the aircraft to take full advantage of the efficiency this configuration theoretically possesses.

Initial Studies – Configuration Drivers and Selection

The RFP specifies a "5000-foot icy runway accelerate-stop distance". After initial sizing, it was shown that an aircraft able to generate and trim out a high lift coefficient on takeoff is required in order to satisfy this takeoff constraint. A low wing loading configuration becomes prohibitive because of high drag it generates during the Mach 0.6 dash. The final aircraft configuration had to be stealthy, efficient and able to takeoff in a limited field length.

It is extremely difficult to create an aircraft which is both stealthy and possesses the high efficiency for the long loiter time required. With shaping being one of the most important ways to achieve a stealth aircraft, planform alignment and sweep are the main methods of providing for a survivable aircraft configuration. The resultant swept, $\lambda=1$, LO-optimized wing has poor efficiency and high induced drag at all positive angles of sweep. An increase in efficiency can be produced by introducing "twist" into the wing in order to modify the lift distribution on the airfoil to be as close to elliptical as possible. Another way, as pictured in Raymer[2] (Figure 4) is to sweep the wing forward, effectively producing both the low-observability and the high-efficiency characteristics desired.

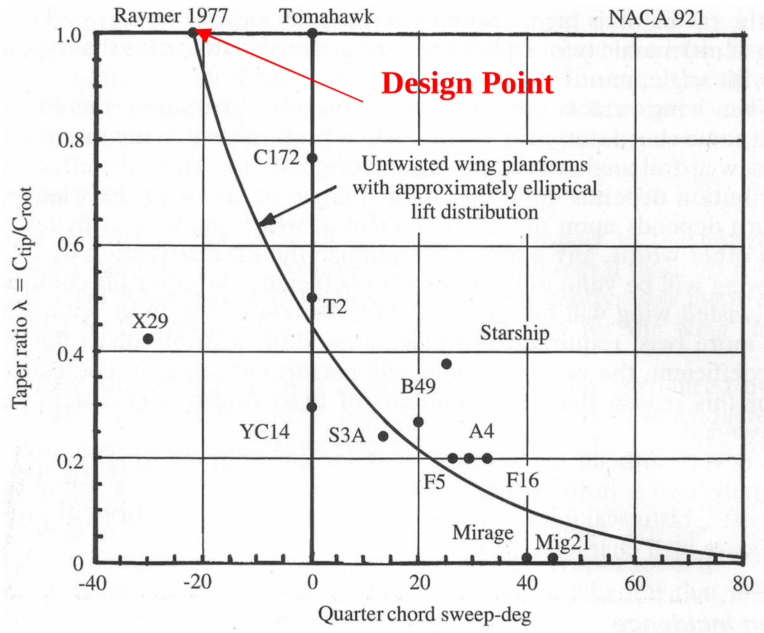

Figure 4 – Sweep Required vs. Taper to Acheive e=1 (NACA 921)

A benefit of a canard configuration is the higher α-oscillation damping provided by the canard/longer fuselage. In conventional aircraft, the high pitch inertia possessed by the fuselage tends to dampen out the pitch oscillation normally developed by the wing. A flying wing with a naturally short fuselage does not benefit from such a damping effect. A high aspect ratio flying wing would likely suffer from this well-known problem of flying wings – the coupling of α-oscillation of the fuselage with wing bending oscillation – which makes control more difficult and places undue stresses on the airframe.

Although the *Predator* system has a wing loading of 26psf and the high static thrust provided by a propeller propulsion system, it still requires a balanced field length of 5,000 ft. The *Predator* can afford to have such a low wing loading – it is not burdened by a Mach 0.6 dash requirement. However, *Molniya* must meet the same field length requirement while using a low static thrust turbofan and still be able to dash out at high speed.

The ground clearance/gear integration advantages offered by this wing configuration are of high importance. Especially on a high-aspect-ratio aircraft such as this, the on-takeoff ground proximity to the tips of a swept-back wing would necessitate a tall set of landing gear and an extremely shallow takeoff angle. As such, the configuration would incur the increased weight and decrease in C_L with the associated detrimental effect on takeoff performance.

Forward-swept wing holds a set of additional advantages to an aircraft configuration. The forward-swept wing allows the wing spar to pass behind the space allocated for the mission payload, creating a more compact aircraft. The proximity of Vloiter to Vstall, is another concern encountered. In case of aerodynamic turbulence, a flying wing flying close to Vstall could easily enter stall with no way to recover. A canard configuration has much higher control authority and, thus, can avoid this problem. Since a fly-by-wire aircraft does not require automatic dynamic or static stability, which has historically been the reason for "conventional" flight controls configurations, more efficient methods of imparting control can be implemented. The configuration is in general more appropriate for an unstable, fly-by-wire aircraft, allowing a decrease of control surface size and actuator power.

Having conducted preliminary static stability and control sizing calculations, it was discovered that the canard located on the nose of the aircraft both destabilized the general configuration and created undesirable RCS spikes. It was theorized that since the tips of both the wings extend as far forward as the nose/canard, the pitch control surface could be relocated to the wingtips.

Having abandoned the flying wing concept because of the takeoff/maximum C_L constraint, the swept-forward blended wing-body configuration was settled on as the final choice. Although the configuration was initially designed as a forward-swept canard, in later iterations it was realized that sufficient pitch control could be achieved using the wingtip control surfaces.

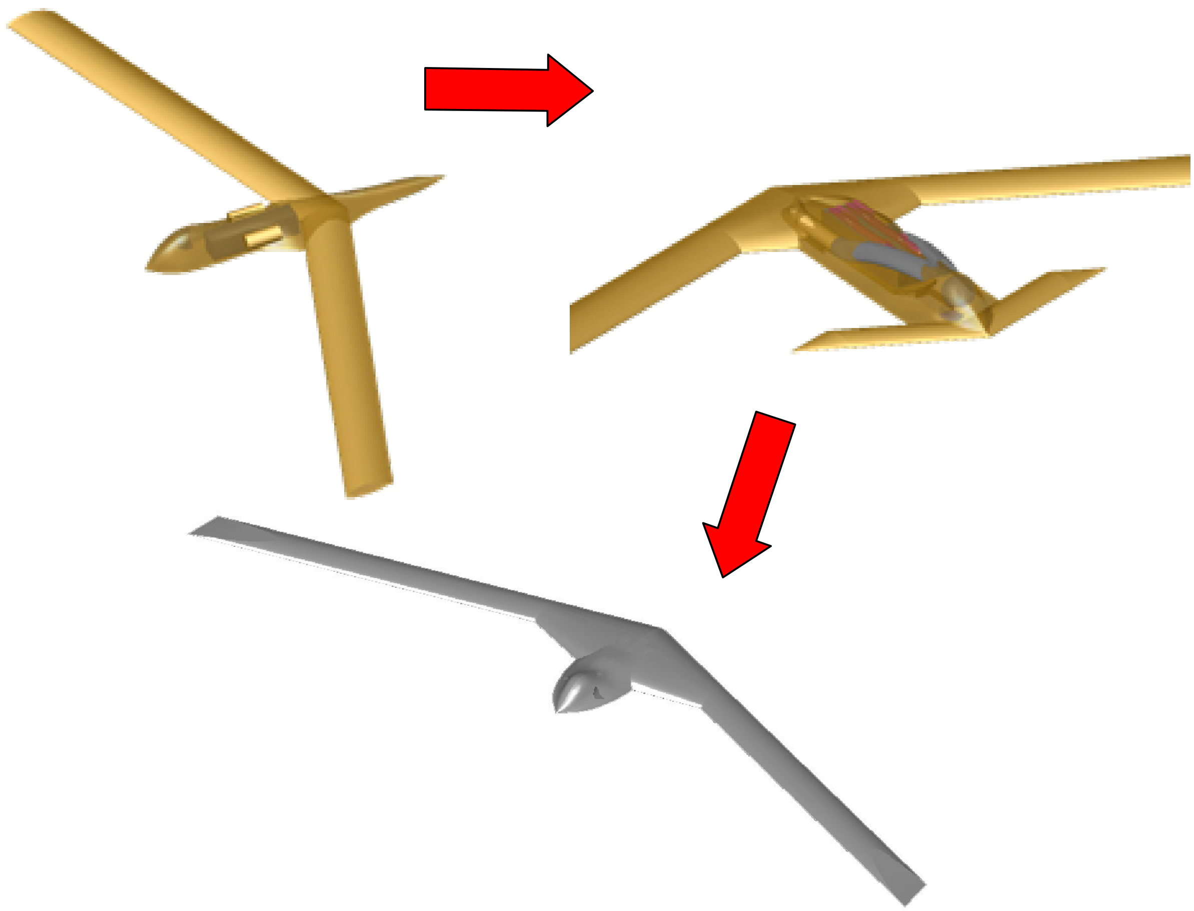

Figure 5 - Configuration Evolution

3.0 – INITIAL SIZING

3.1 – Parasite Drag

In order to estimate aircraft drag during various flight regimes, the program FRICTION was used. Using a simplified aircraft geometry input file, parasite drag coefficients were estimated at various Mach numbers and altitudes. Since both laminar and turbulent flow regimes are simulated, flow transition points were be specified. The program also accounts for the effects of airfoil thickness. The coefficients output by the program were used to approximate the parasite drag of the configuration during mission simulation. The drag coefficients were interpolated in order to find a C_{D_p} at every point of interest.

Table II – Parasite Friction Coefficients

Altitude (ft)	Mach #	C_D Friction	C_D Form	C_{D_p} Total
25,000	0.2	0.00511	0.00199	0.00710
25,000	0.4	0.00433	0.00169	0.00602
35,000	0.6	0.00422	0.00165	0.00586

3.2 - Mission Simulation

The aircraft was sized using an integrated mission simulation spreadsheet program. With Microsoft Visual Basic, a range of aircraft configurations could be run through a mission profile, and the performance of each analyzed with a common set of tools and assumptions. Upon recognizing a viable configuration, the spreadsheet program decreased the takeoff gross weight, which affected the weight/size of most other components, in order to find the minimum for that configuration. This way, wing loading, aspect ratio, engine thrust and other aircraft size drivers could be optimized with a much higher degree of fidelity compared to that of simple constraint plots, while maintaining a fast configuration evaluation turnaround time.

The spreadsheet program incorporated separate modules for weight calculation of each potential configuration. The performance of the aircraft was calculated during the 5 main mission segments: Takeoff/Climb, Cruise In, Loiter, Assess, Cruise Out, Reserve. The spreadsheet program optimized velocity for loiter, maintaining the best L/D speed throughout the mission. Climb was performed at the best speed-to-climb velocity. Besides cruising at V_{BR}, cruise climb was implemented to investigate its effects on lowering fuel consumption.

The program accelerated the development process of the *Molniya* concept dramatically, allowing the project to go from start to a finished design in roughly a month's time.

3.3. Propulsion

3.3.1. Engine Simulation

One of the major sticky points that occurred during the design process was caused by the lack of available modern small-size turbofan performance data. With the 1000+lbf thrust level turbofan market being a very competitive one, most manufacturers were reticent to provide the performance data for their engines. Inquiries made at Pratt and Whitney, Agilis and Williams all resulted in little hard performance data. Lacking precise performance data, a different approach had to be undertaken.

An engine deck was available for an early 1990s Williams FJ44 engine – a close relative of the FJ33, one of the more modern engines evaluated for use in *Molniya*. This deck was scaled to achieve the thrust values necessary for the rubber engine methodology that was used throughout the design process. Not possessing detailed engine data for other engines, the FJ44 was considered to be representative of the level of early 1990s technology in small turbofan engines. The implementation of a scaled engine map was considered a more realistic approach than using generalized turbofan performance equations. A 3-D interpolation routine was used to acquire realistic values of fuel consumption from inputs of thrust required, Mach number and altitude. Once again, it should be noted that using an integrated design tool allowed for more realistic mission performance simulation than the standard fuel-fraction method of aircraft sizing.

Lacking the SFC values for the FJ33-generation of engines, the first sizing run was performed using the SFC values directly interpolated from the FJ44 levels. Being applied to the long-duration mission, this SFC assumption drove the aircraft weight up considerably; the optimum aircraft design point of that run being located at the 15,300lbf takeoff weight mark.

Although still lacking precise data to estimate SFC levels for an FJ33-class engine, it was suspected that the SFC of such an engine was lower than the direct interpolation of the FJ44 used in the initial sizing run. The FJ33 has a higher overall compression ratio, a direct driver of engine efficiency and its certification date is a decade later than that of the FJ44, allowing it to make use of new technology. The SFC ratings (only 2 quoted, no map) for a more modern engine, such as the Agilis TF-1200 were much lower than those for the FJ44. Finally, company chairman and CEO Dr. Sam Williams described the FJ33 as "a step beyond the FJ44" in terms of thrust-to-weight ratio and performance.[3] Because of these reasons, it was decided that modification of the assumed SFC for the modern small turbofan had to be implemented.

According to the RAND Corporation, "Overall pressure ratio (OPR) is the dimensionless ratio of the pressure of the air exiting the high-pressure compressor to the pressure of the air entering the fan on a turbofan engine, or entering the compressor on a turbojet, turboprop, or turboshaft. High OPR contributes to high engine efficiency and, in turn, low SFC."[4] The SFC ratings of the FJ44 base engine were modified according to the engine OPR trend line that can be seen in figure 5.

Based on the trend line shown in Figure 6, the OPR for the FJ33-class engine should be roughly 12% lower than that for the FJ44-class engine. When SFC values of the FJ44 were modified to reflect this trend, they ended up being slightly below to the predicted SFCs for the newer TF-1000 engine, thus showing that the scaling methodology implemented is legitimate.

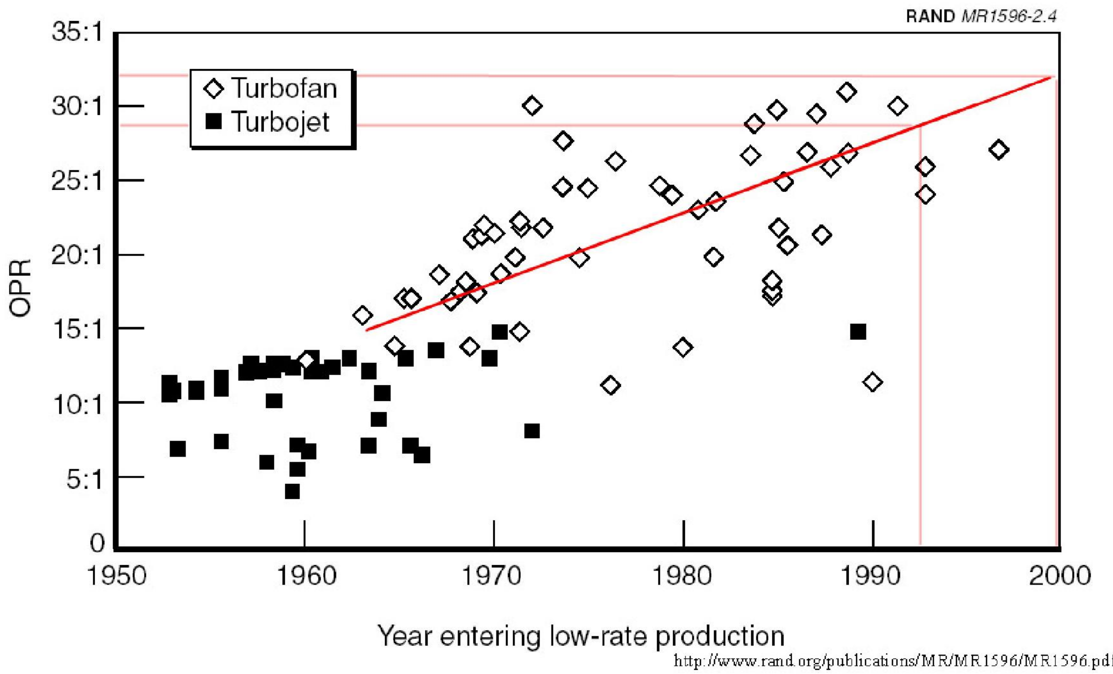

Figure 6 - OPR vs LRP Year

Having derived an approximate SFC level for a small 2003-level turbofan engine, the aircraft sizing process could begin. The SFC data used in simulation can be seen in Attachment A.

3.3.2. Engine Configuration

The sizing program was used to evaluate the differences between a single and twin-engine configuration. The twin-engine configuration seems to offer a set of benefits. With the total thrust of the aircraft being sized by the Mach 0.6 dash and the takeoff constraint, excess thrust is present during the low-speed loiter. One of the two engines could be shut down during the long-duration loiter so that the high-thrust, low-SFC operation of a single engine would contribute to a reduction of the total fuel flow. Many long–endurance aircraft use this approach to extend flight times. Both the P-3 Orion ASW aircraft and the Voyager record-setting aircraft turned off their engines to decrease specific fuel consumption in long-duration flight. The twin-engine configuration also offers a higher degree of safety by allowing the aircraft to return to base in case of an engine failure or battle damage.

In order to numerically compare the performance benefits of single and twin-engine configurations, a range of configurations was evaluated using the sizing program. The results of this study can be seen below in Figure 7. It can be seen that for configurations of equivalent total installed thrust, a twin-engine configuration has a gross weight that is much lower that of a single-engine configuration. If the trends portrayed in the single-engine carpet continue, it appears that a viable single-engine configuration would have a gross weight of roughly 19000 lbs.

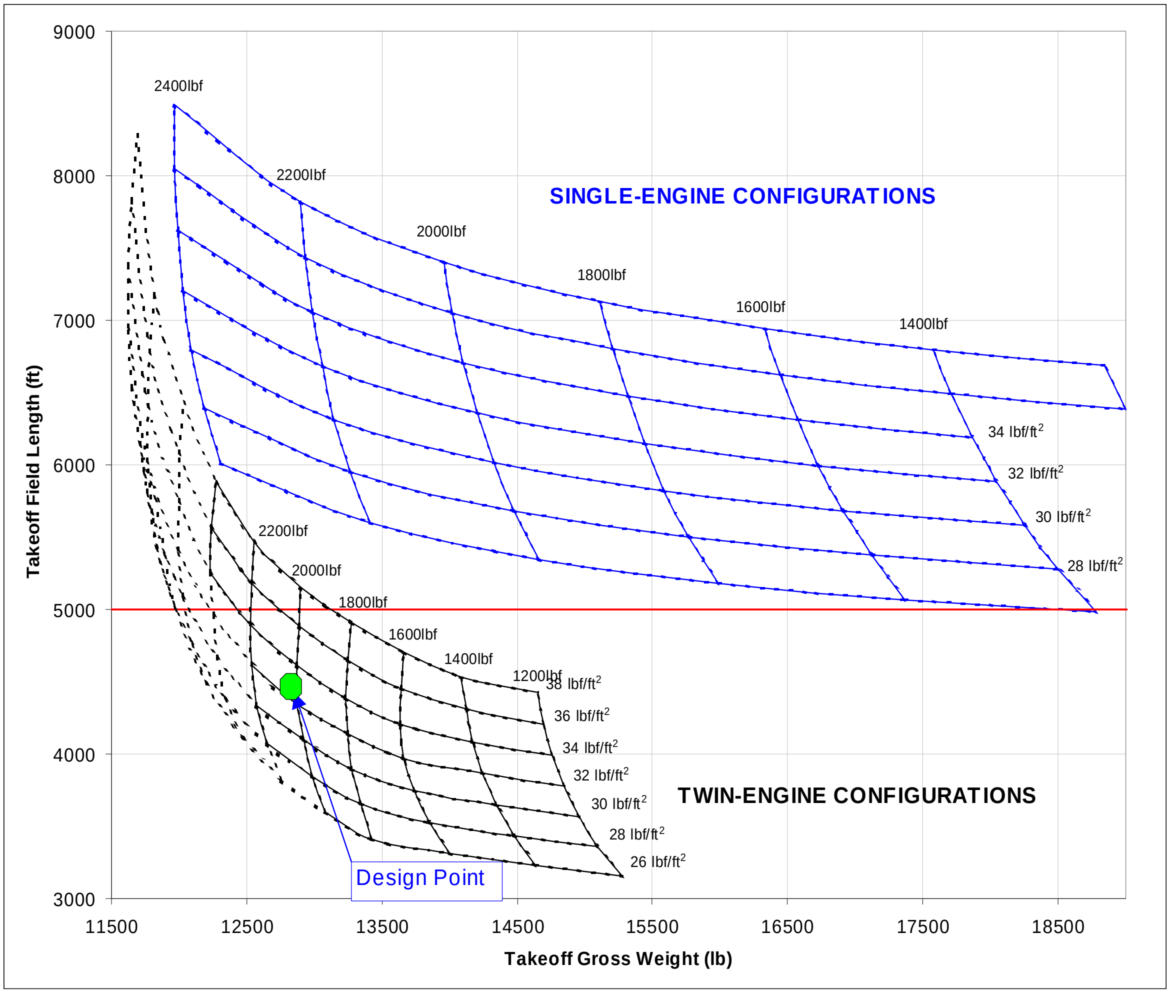

Figure 7 - Engine Number Trade Study

3.4. Aerodynamics

3.4.1. Maximum Lift Coefficient

With the three configuration drivers being the 0.6 Mach dash, the 5000 ft takeoff constraint and the 35-hour loiter time, a sizing trade had to be conducted to optimize the wing area/maximum C_L for the aircraft configuration. This trade is a good example of the power of the sizing program developed for the design of the *Molniya*. A plot in Figure 8 below shows the aircraft sizing trade for a set of configurations, for which wing loading, installed thrust and takeoff C_L were iterated. The 5,000 ft. takeoff accelerate-stop distance and drag generated by the high-area wing at Mach 0.6 constraints can be seen limiting the number of viable configurations.

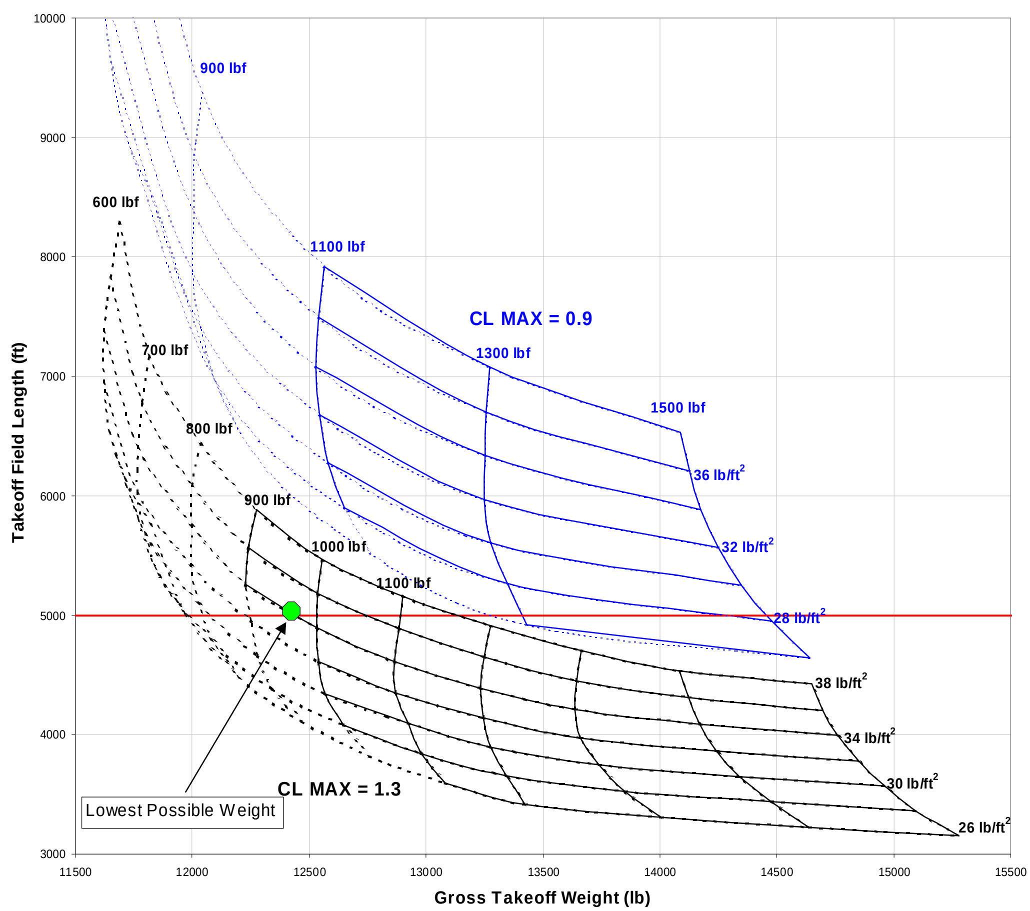

Figure 8 - Wing $C_{L_{MAX}}$ vs. Gross Weight

This trade study clearly shows the dependence of the general aircraft configuration and of the gross weight of the aircraft on the maximum C_L that can be achieved.

The C_{Lmax} =0.9 and C_{Lmax} = 1.3 configurations are representative of swept-back flying wing and conventional configurations, respectively. A conventional or a canard configuration is able to create the trimming moment necessary to maintain pitch stability during takeoff, while the flying wing configuration, lacking a way to trim out the high moments generated by deployed high-lift devices, suffers from a markedly low maximum C_L capability. The 0.9 Max. trimmable C_L configuration shown in the plot is a value of the C_L capability of a typical high-AR flying wing configuration at the low Reynolds numbers encountered by a UAV during takeoff/landing. Trimming out a high C_L on a flying wing requires a negative elevon deflection, an action that decreases the overall lift even further. A C_L of 1.3, however, is considered easily obtainable for either a conventional, canard or a forward-swept configuration. As such, the trade study shows that a high-C_L configuration could be built approximately 1000 lbs lighter than a flying wing configuration. Being able to trim out a high C_L value becomes more important when once considers the inevitable weight growth that operational aircraft undergo, and the fact that in the two configurations presented above, only one can be easily modified to increase C_L max. A general aircraft study trade at the selected wing C_L max can be seen in Figure 9 below.

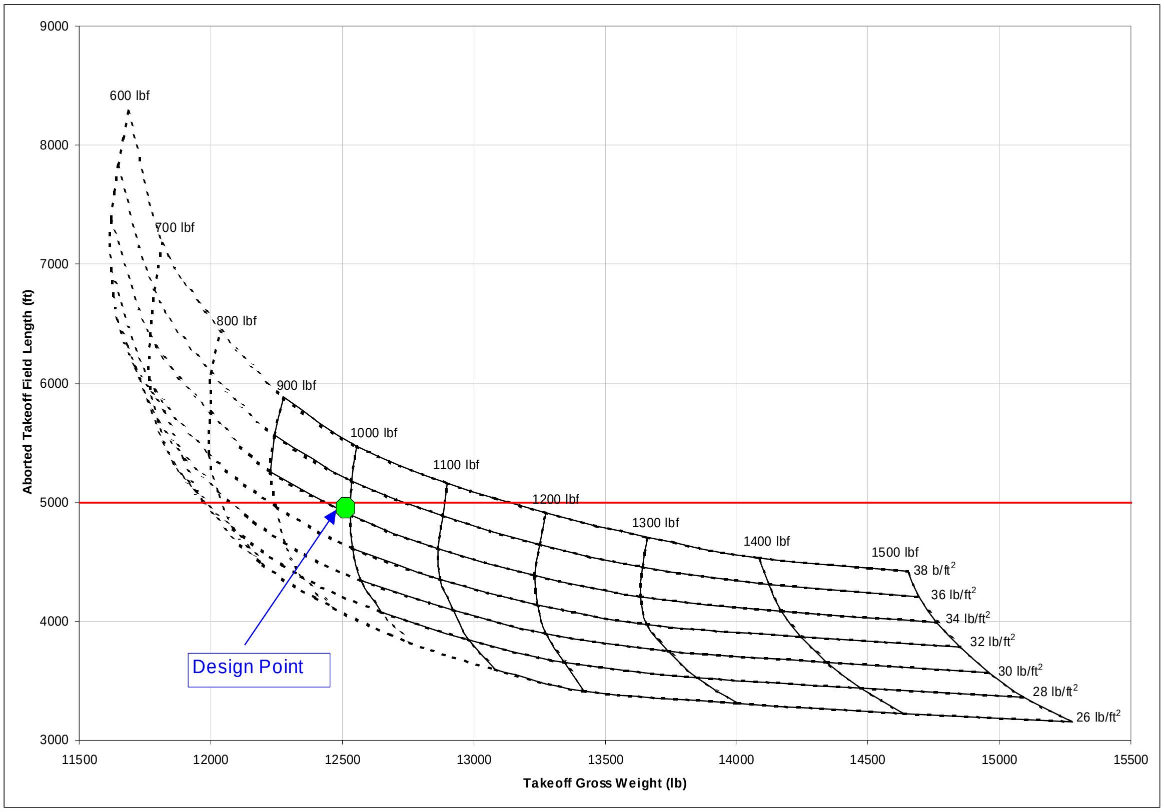

Figure 9 – Installed Thrust vs. Wing Loading Trade

4.0 – PRELIMINARY DESIGN

4.1. Aerodynamics

4.1.1. Airfoil Selection

Resultant from the best velocity optimization used in mission task simulation, the following C_L values were used during the various regimes encountered by the aircraft.

Table III - C_L Ranges During Mission

Flight Segment	C_L Range	Time Spent
Cruise Out	0.420	.5 Hours
Loiter	0.63-0.60	35 Hours
Cruise In	0.42-0.40	.5 Hours

Maximum L/D is obtained when parasite and induced drags are equal: being able to obtain measurements of induced drag from the planform/aspect ratio of the aircraft, the speed required for maximum L/D was obtained. An airfoil having a pronounced drag bucket at the average C_L values and loiter Reynolds number range encountered during the loiter segment was the TH 25816 HALE airfoil developed by Doug Hall at the Naval Air Development Center (Ref. Figure 10).

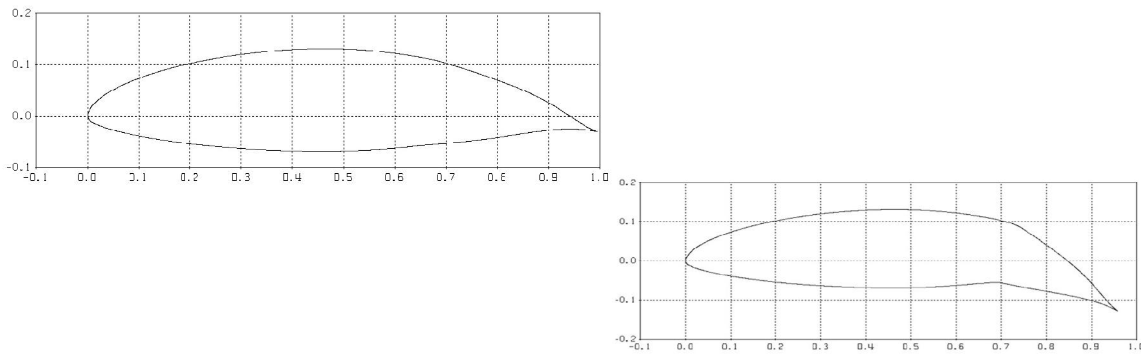

Figure 10 – TH 25816 HALE Airfoil: Unflapped and with 20° of flap

This airfoil was chosen not only because of its low-drag qualities but also because of its high thickness-to-chord ratio (t/c). Because the high aspect ratio wing of *Molniya* is not only forward-swept but also carries large amounts of fuel, it requiring a high degree of torsional stiffness, a high t/c airfoil was an obvious choice. Some modifications were made to the airfoil, lowering its thickness to 18% in order to reduce the drag produced during the Mach 0.6 dash, and increasing its camber to 5% in order to increase the maximum lift coefficient of the airfoil. Considering that the maximum Mach number *Molniya* achieves is Mach 0.6, the decrease of thickness to 18% was expected to practically nullify compressibility drag effects. (Ref. Figure 11)

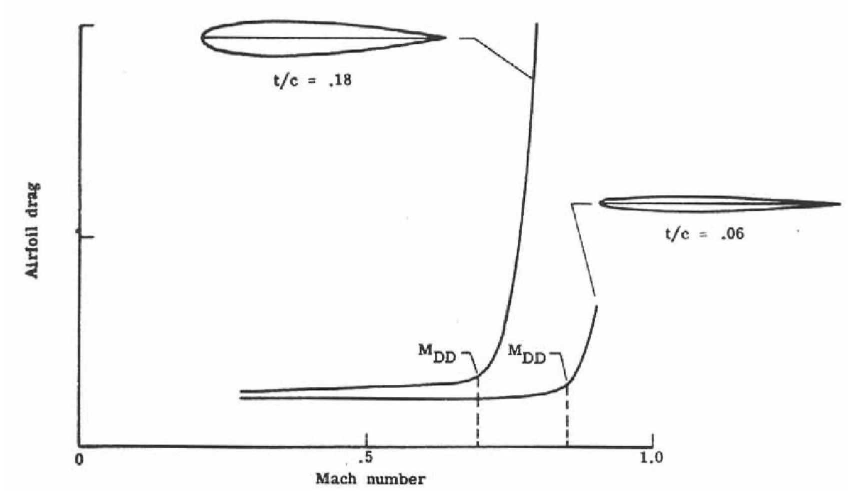

Figure 11 – Compressibility Drag Effects vs. Mach Number

A plot comparing the performance of the two versions of the TH-25816 can be seen in Figure 12 below. It can be observed that the modified airfoil achieves the cruise C_L of ~0.7 at a much lower C_D value than the original TH-25816, but at an expense of generating a slightly more negative moment coefficient. This higher moment coefficient can be dealt with by incorporating an active fuel management system into the aircraft. The forward-swept flying wing configuration is also beneficial in trimming out this moment coefficient by creating higher lift at the tips.

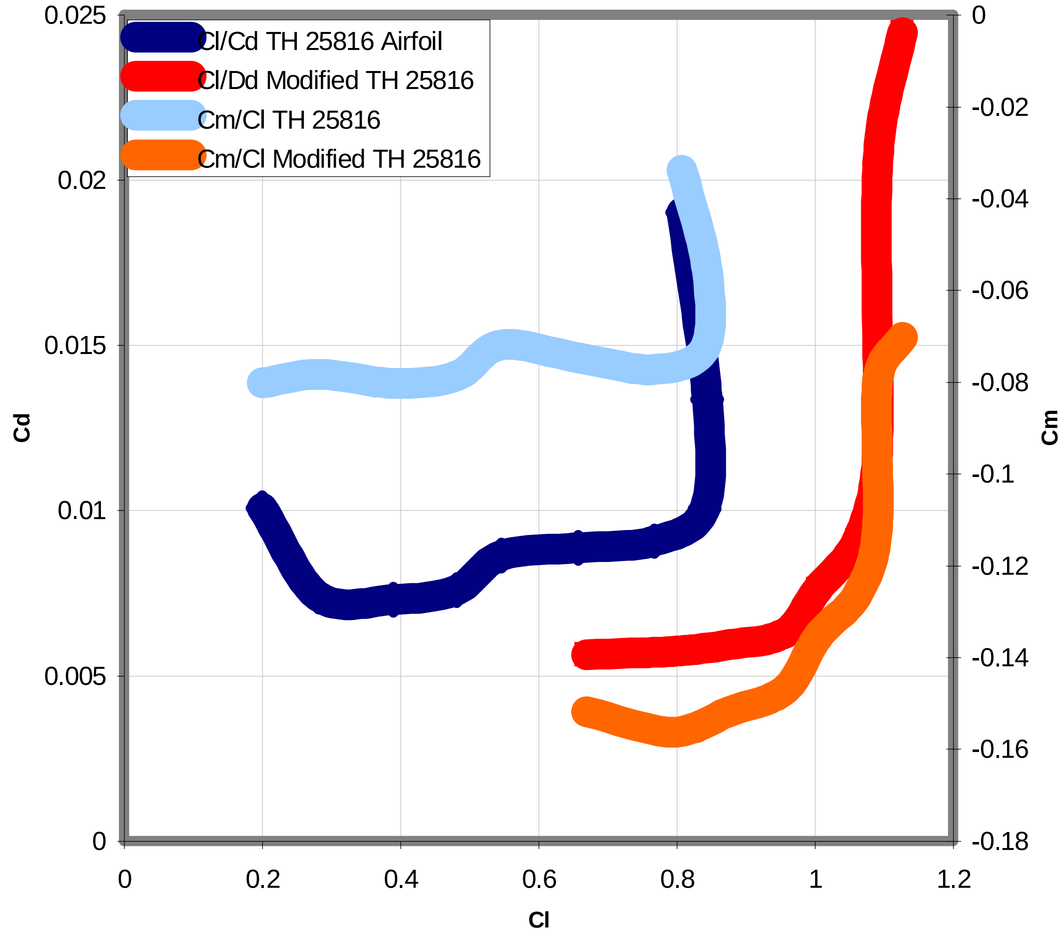

Figure 12 – Comparison: TH25816 and Modified TH25816 at Re=3x10^6

4.1.2 – Airfoil 3-D Lift Curve

The 3-D lift curve and the induced drag generated were approximated using the Oswald's efficiency factor. Oswald's efficiency factor, e, was a combination of software output from the LamDes program described below and a real-life modification factor to account for the non-optimum lift distribution generated by the fuselage.

4.1.3 – Planform

The planform of the aircraft was optimized using the program LamDes which can be freely downloaded from W.H. Mason's website. The program was used to evaluate the planform Oswald efficiency and to find the spanload that would minimize the sum of the induced and pressure drag at the loiter C_L. A high degree of importance for use in the design of *Molniya* was the software's capability to find the minimum trimmed drag of a configuration while satisfying a pitching moment constraint. This allowed the optimization of the *Molniya* planform for the loiter mission segment.

The geometry presented in Figure 13 was input into the program. The program output a span efficiency of 1.0; however, to account for non-ideal lift distribution over the fuselage/wing joint, a value of 0.85 was used in simulation.

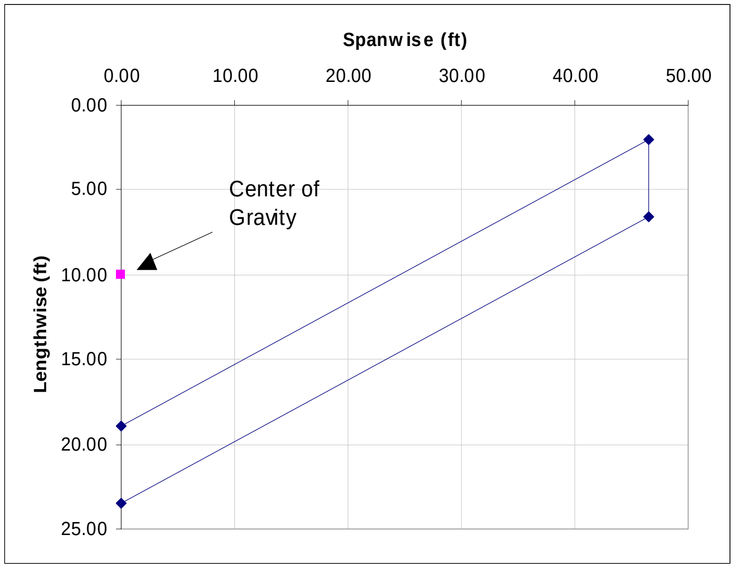

Figure 13 - LamDes Geometry Input

4.2. Structures

One of the most crucial considerations in the design of *Molniya* was the forward-swept wing design. This unconventional configuration has traditionally been ignored, in spite of its aerodynamic and packaging benefits because of the structural problems it introduces. However, during the recent years, a wide range of aircraft built using modern composites technology has proven that a forward swept wing is no longer an insurmountable obstacle. High-speed aircraft such as the Sukhoi S-37 have been tested with low-aspect-ratio, high G-loading forward-swept wings. A much higher AR forward swept wing can be seen in the successful *Boomerang* aircraft created by Scaled Composites (Figure 14).

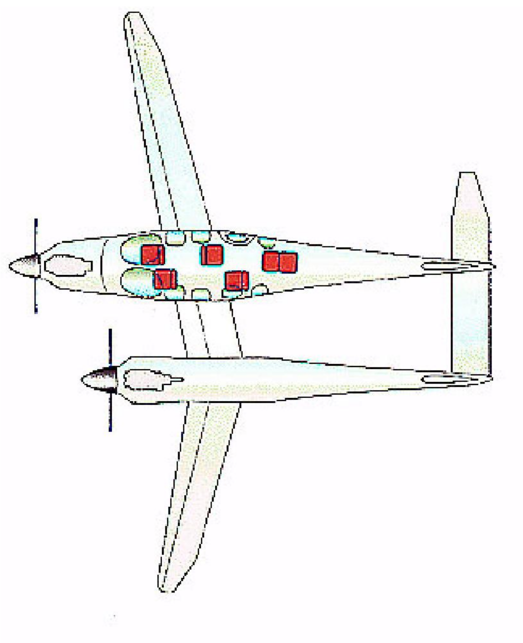

Figure 14 - Scaled Composites *Boomerang*

Using modern composites manufacturing technology, it becomes possible to build a structure with focused directions of stiffness. Using this technology, a wing that naturally washes out as it bends upward can be constructed. The X-29 aircraft produced this effect by a combination of spar and wing skin design. The forward spars are made out of titanium, while the rear spars are of much more flexible aluminum. With the carbon fiber top and bottom skins of the wing fiber lay-up tailored to twist when bent by aerodynamic loads, a non-divergent forward-swept wing was constructed. The main spar is positioned closer to the leading edge at the tip of the wing than at the root. The combination of all these features causes the wing to naturally increase washout when it bends up, reduces the angle of attack at the tip and stops the runaway bending from occurring.[5]

Although it is difficult to test the validity of this assertion with the quantitative tools currently available to the designer, the real-life examples of successful forward-swept wing aircraft mentioned reinforce the validity of the design choice made. Many low-impact active control methods could be used to deal with the divergent behavior of the wingtip.

When estimating the weight of the structural components of the aircraft, the G-loadings specified in the RFP were applied to all components with parametric equations able to accept such input.

4.3. Propulsion

In order to satisfy the RFP's takeoff constraint requirement, a trust reverser system had to be used to help braking on the icy runway. The RFP specification of an "accelerate-brake" distance was interpreted to apply all types of aircraft. A twin-engine aircraft such as *Molniya*, having sufficient power to continue with an OEI takeoff would not be exempt from the requirement and would have to be designed to have the specified 5,000 ft stopping distance.

Although it would have been preferable to join the two intakes into a single one, such a configuration did not materialize because of the space constraints – with the engine location being dictated by CG reasons, the intakes could not be brought together quickly enough. Instead, a set of twin intakes are used, one on each side of the fuselage.

Because of the aircraft's operational practice of turning off an engine in mid-flight, the intakes had to be fitted with mechanically operated "covers" to be deployed upon engine shutoff. The cover was necessary to prevent the shut-down engine from generating excess drag and yaw moment.

The configuration of the exhaust system of the aircraft was challenging both because of the spatial but also because of the low-observability constraints. Being able to provide for symmetrical thrust during one-engine loiter condition, was a big point of concern. To accomplish this, the exhausts of the two engines had to be smoothly connected together into one nozzle coming out of the back of the aircraft.

Having finalized the sizing of the aircraft, an optimum design thrust point was established at a 2x1000 lbf mark. The Agilis TF1000 engine fit the requirements perfectly; in fact, the SFC levels quoted on the company's website were slightly better than those used in the simulation, giving the results achieved here a good margin of safety. It should be noted that the TF1000 engine is an in-development engine which is on schedule to have its first run within the year. The design point picked will allow the configuration to move to the off-the-shelf FJ-33 (2x1200 lbf) engine configuration in case the development of the TF1000 does not meet its performance expectations or suffers unexpected delays. The two configurations can be seen in Table IV. The aircraft will have to undergo a minimum amount of modification, with the fuel volume necessary increasing by only 8ft^2. Keeping this solution in mind, the configuration presented in this report will focus on the Agilis TF1000 engine.

Table IV - Possible Aircraft Configurations

Preferred 1000 lbf TF1000 Engine		**Contingency 1200 lbf FJ33**	
Wing Span	83.7	Wing Span	83.7
Wing Chord	4.2ft	Wing Chord	4.2ft
Wing Area	367.6ft2	Wing Area	367.6ft2
Aspect Ratio	20.0-	Aspect Ratio	20.0-
Sweep	20.0deg.	Sweep	20.0deg.
GTW	12500.0lbs	GTW	13000.0lbs
EW + PL	5804.3lbs	EW + PL	5963.0lbs
Fuel WT.	6695.7lbs	Fuel WT.	7037.0lbs
Drag Area	467.6ft2	Drag Area	467.6ft2
W/S	34.0	W/S	34.0
Final Fuel Weight	2.6lbs	Final Fuel Weight	6.6lbs
Tmax Used	139.4% max	Tmax Used	118.1% max
Icy RTO Dist.	4884.2ft	Icy RTO Dist.	4493.4ft
Fuel Volume	131.6ft^3	Fuel Volume	138.3ft^3
Range	7546.1Nm	Range	7693.9Nm

4.4 – Low Observability

4.4.1. RCS

Because the *Molniya*'s design mission includes loiter and attack of enemy air defense assets, it was natural for the aircraft to incorporate features of stealth technology. Some of the most noticeable features of the geometry of *Molniya* are the product of geometric shaping being used to lower the radar cross-section (RCS).

Planform alignment was used on all of the air vehicle, creating its untapered forward-swept main wing configuration. All of the leading and trailing edges of the aerodynamic surfaces are aligned to have radar generate radar energy reflection spikes 20º off the centerline of the aircraft. The sides of the aircraft are canted at a 55º angle to bounce radar energy away from the source. Although this particular angle of sweep is dictated by aerodynamic efficiency, it was also evaluated to place radar spikes well away from the source in both the attack and in loiter orientations. The results of the RCS sweep of the aircraft can be seen in Foldout B. It can be seen that a set of spikes is generated by the airframe at 20º both fore and aft, but that the RCS as observed at 90º is as low as that observed from straight-ahead. Because of the locations of these low-RCS directions, *Molniya* will be able to not only attack enemy radar installations but also loiter in the vicinity without being detected by radar.

In order to analyze the radar cross-section of *Molniya*, a solid model was evaluated using the Radbase2 software from Surface Optics. Having faceted a model in 3D Studio Max, (Ref. Foldout 2) a set of calculations could be performed.

RadBase is a fully validated, commercial off-the-shelf (COTS) software system, developed by Surface Optics Corporation (SOC), for generating accurate Radar Cross

Section (RCS) and Amplitude and Phase data for both complex targets and cultural features.[6] Having input the frequency of interest (XX, XX GHz), the incident angles (0º, 15º) and having limited the number of bounces to #, the aircraft geometry was analyzed.

The code performed calculations at 1º azimuth increments at the two incidental angles specified. The frequencies of interest were chosen on the basis of those used by radars of Russian surface-to-air missile systems which are presented in more detail in Foldout B. Although the missile systems presented are known threats to both manned and unmanned aircraft, reliable information enabling quantification of their relative danger is unavailable. Because of this, the level of LO required to perform the RFP mission could not be accurately predicted; and the design had to simply focus on minimizing the signature of the aircraft until the cost or performance tradeoffs got too high.

The 0º angle of elevation was evaluated to simulate detection by fighters and enemy AWACS assets. At *Molniya's* 25,000ft loiter altitude, most enemy ground systems will observe the aircraft an angle of roughly 15º. Because the main role of *Molniya* is ground observation and attack, it is most important that it have low radar return in that direction. By shaping all the aircraft sides to be parallel, *Molniya* sends a radar energy spike away from the source unless it is directly overhead.

The communication antennas present in every modern aircraft have a large potential for creating reflections that will be cause an otherwise LO aircraft to be visible to enemy radar tracking installations. Making *Molniya*'s radar and antenna installations as low-observable as possible is necessary. Since few of the technologies used to shield the antennas on stealthy aircraft are in public domain, more detailed research has to be conducted on this subject. At a minimum, the use of bandpass resonant radome covers will be necessary.

Passive stealth is not the only way to ensure the survivability of the aircraft. Chaff, flare and active jammers are all likely to be useful for employment on *Molniya*, however they are likely to be used as a last resort and not considered to expand the weapon system’s capability any.

4.4.2. Infrared

Achieving low observability in the infrared spectrum is just as important for *Molniya*'s mission as achieving low RCS. Although no SAMs capable of reaching *Molniya* at its cruise altitude target IR emissions, a wide range of modern air-to-air missiles home in on their target's IR signature. In order to obtain the "balanced observability" characteristic of the *Molniya*, the level of these emissions had to be reduced to that appropriate for a LO aircraft.

The RFP specifies that the aircraft be designed to have balanced low-observable characteristics. In order to ensure this, infrared emissions of the aircraft must also be minimized. This will be done by matching the IR emissivity of the airframe to the surroundings by application of special paints and coatings to areas of concern. The exhaust of the core of the engines will be routed through a long duct where the bypass and core gases will be mixed. The exhaust is also located in such a way as not to be visible by radar sources located on the ground.

A problem which occurs with prolonged exposure of an aircraft surface to exhaust gases is the accumulation of carbon deposits that occurs in that area. Carbon is one of the best possible materials to radiate in the IR spectrum and negatively affects the stealth characteristics of the aircraft. As can be evidenced by the more recent stealth aircraft developments (*Bird of Prey*, X-45), it seems more advantageous to locate the exhaust nozzle at the very end of the fuselage.

4.4.3. Visual

Little data and practice exists on the techniques of visual stealth, but at the minimum, the painting of the aircraft's body in a "low observable" color scheme is the least that must be done. Active visual stealth techniques are not yet prospective enough to be used on an operational aircraft. Techniques such as the light color area used to mask the intake on the *Bird of Prey* aircraft (Figure 15) will have to be used to provide Molniya with higher survivability during daylight operations.

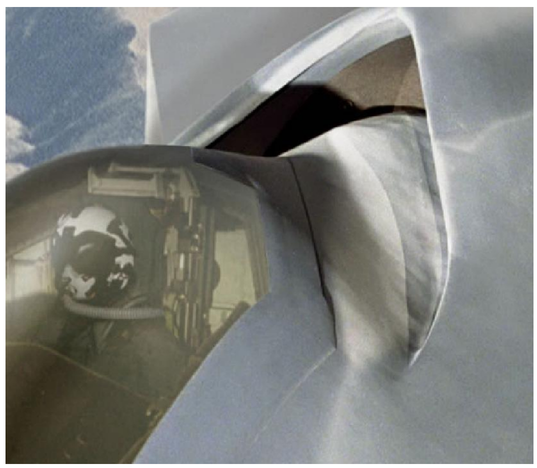

Figure 15 - *Bird of Pr*ey Intake

4.5. Sensor Integration

An IR sensor system with a NIIRS[7] rating of 6 is likely to be necessary for accomplishing the basic surveillance/light attack mission of the aircraft. The conventional IR system of such capability that is currently used on the *Predator* aircraft can be seen pictured in figure 16.

Figure 16 – Raytheon AN/AAS-44 FLIR

Besides providing high resolution imagery, a stealthy and low-drag installation of the sensor was also paramount to the aircraft's mission. A alternative system presented itself in the *SniperXR* technology by Lockheed Martin, a new-generation FLIR pod being integrated with the F-16 and the F-35 aircraft. The downside of that particular system is the limited field of view offered by it. Having been designed for strike-only aircraft, the pod does not offer a 360º azimuthal field of view, which makes it less than ideal for surveillance applications. Upon evaluation of the modification used in the F-35 fighter, it appears that the field of view of the sensor is limited only by the shape of the sapphire window of the low-observability enclosure. If a different window were to be manufactured, the *SniperXR* EOTS could easily be used on *Molniya*.

Figure 17 – F-35 EOTS Window

Making full use of the technology already developed for the JSF program, a DAS (Distributed Aperture System) thermal imaging system is also installed on the aircraft.

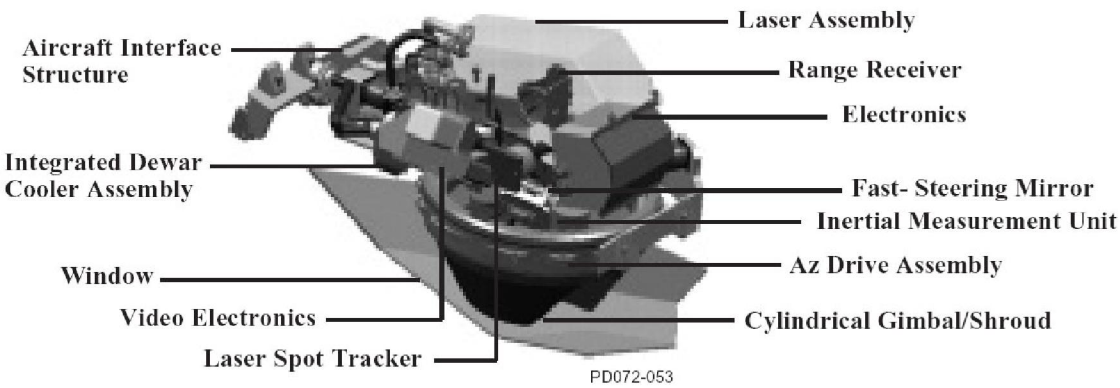

Figure 18 – Internal components of the JSF EOTS system.

This system provides *Molniya* with 360° situational awareness as well as navigation, missile warning and IRST functionality. A window shape that would be ideal for the *Molniya*'s purposes is pictured in Figure 19.

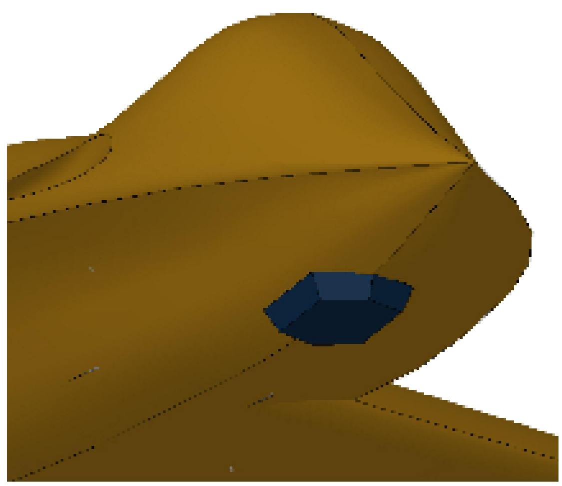

Figure 19 – *Molniya* EOTS Window/Location

The EOTS sensor is ideally located in a point on the airframe which minimizes the view area blocked by airframe components. In order to achieve the best field of view, the EOTS sensor was located on the lower centerline of the aircraft's nose. This location allowed an uninterrupted 360° azimuthal field of view for the sensor. The center-mounted sensor window created an interference with the traditional location of the nose landing gear. To accommodate the sensor requirement, the landing gear leg was offset to the right and mounted asymmetrically on the aircraft underbody.

4.6. Electronics Payload

The electronics payload package could include a wide array of systems. Although no specific system was specified in the RFP, the aircraft has to be designed to be able to incorporate a wide number of possible payloads. The electronics payload package was not specified by the RFP and could theoretically include a wide array of systems. Being constrained by the payload capability of the *Molniya*, the likely candidates are LYNX[8] or the SAR payload from the Global Hawk UAV.

Housing certain types of electronics payloads, such as a side-looking radar necessitates that the sides of the payload bay be transparent to the payload's radar emissions. Because of *Molniya*'s relatively low loiter altitude, the SAR payload will need to have a shallow observation angle in order to scan the maximum amount of area. Most modern SAR payloads implement side-looking radar sensors, the field of view of which will likely interfere with the structure of a flying wing aircraft. Interference of the mechanisms operating a standard payload bay configuration area are also a concern.

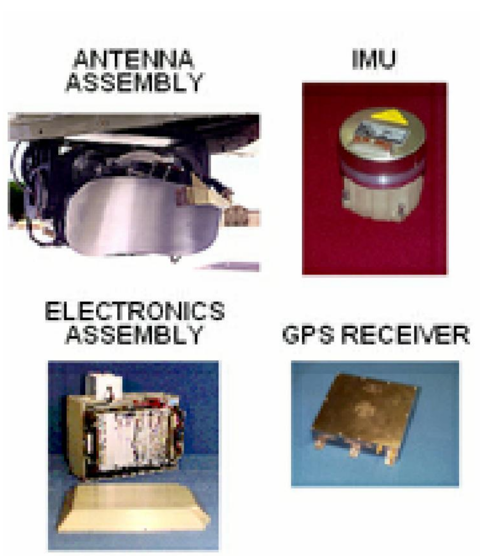

Figure 20 – LYNX

4.7. Landing Gear Configuration

The integration of the landing gear into the aircraft could proceed once a center of gravity was estimated with enough precision. Because of the planform configuration of the aircraft, locating the main gear contact patch at the recommended 15° angle from the center of gravity proved to be impossible because of structural constraints. The main gear leg has to attach to a load-bearing structure within the wing, and that can only be accomplished using a mounting method shown in Figure 21 below.

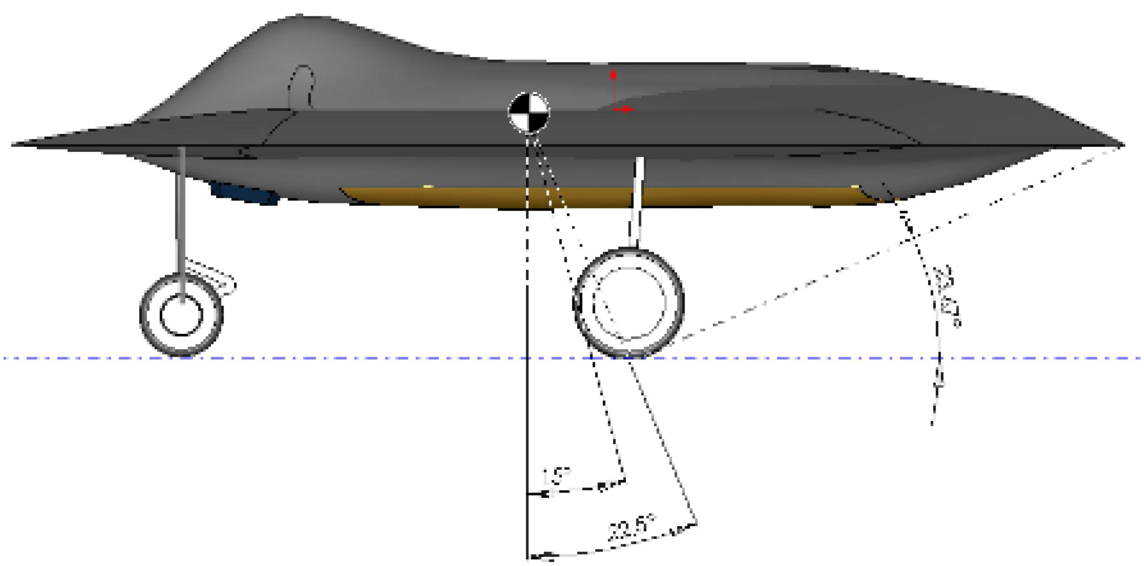

Figure 21 - Main Gear Location in Relation to the CG

The main landing gear is positioned at an angle to the vertical in order to span the distance between the ground contact point and the gear mounting location on the wing spar. The gear in its stowed arrangement can be seen in Figure 22.

Because of its retraction geometry, size and design loads, the main landing gear from the F-5 fighter aircraft made a good choice for use in *Molniya*. For initial prototype production, it is often advantageous to use an off-the-shelf system, as demonstrated by the use of this landing gear in the X-45 technology demonstrator.

As mentioned earlier in the text, the nose gear had to be offset to the right as not to interfere with the FLIR/EOS view window located directly in the front of the aircraft. This slight asymmetry is unlikely to cause any sort of handling problems for the aircraft, a similar type of landing gear configuration being used in the A-10 *Thunderbolt II* aircraft.

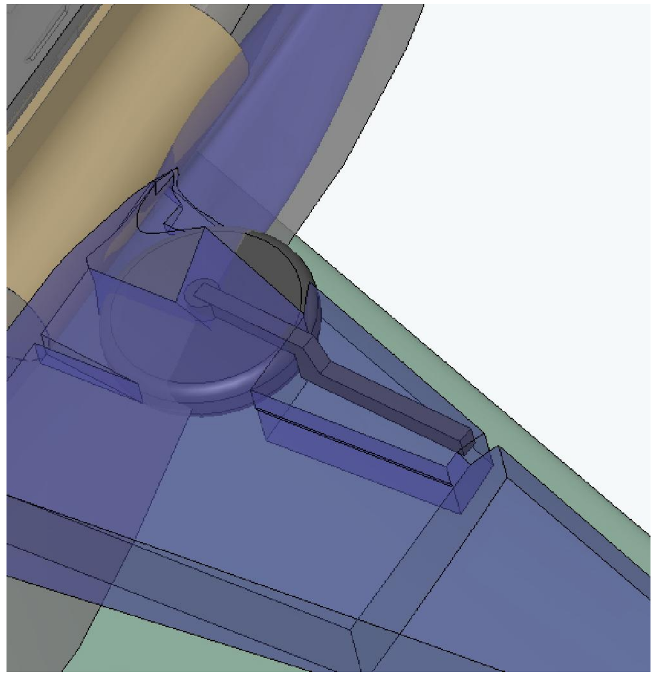

Figure 22 - Stowed Main Landing Gear as Seen From Above

4.8. Weapons Configuration

Various types of missile arrangement were deliberated upon, but as the mission specified a 8ftx2ftx2ft electronics payload, it was only natural to fit the two other payloads within the space defined by that requirement. An interesting issue arose when a weapons deployment scheme was considered – because of the “square” arrangement of the 4 *Hellfire* missiles, it would be difficult to deploy them via the traditional “ejector rack” – actuators for both the bay doors and the 2x2 “rack” extension mechanism would be required. This configuration would also be compromised by a poor RCS when extended. A rotating door/missile mount or a “platform” configuration were the other ideas considered for weapons deployment.

The rotary door configuration would require more fuselage space because of the clearance issues pictures. Another constraint arose when one the mission of *Molniya* was compared to the types of weapons specified in the RFP. Both the *Maverick* and some models of the *Hellfire* require for the seeker to “see” the target before launching. This constitutes a problem, considering the missiles are far from stealthy. Obviously, a launch must be conducted as quickly as possible to reduce the time the aircraft is exposed, but shielding the payload in the “deployed” configuration would definitely reduce the risk to the launching aircraft. As such, the “platform” configuration could have RAM-treated sides covering the missiles at little or no weight penalty, reducing the RCS of the “deployed” configuration aircraft. The lack of a permanent “payload bay door” would also simplify the integration of a custom sensor package – allowing the aircraft underside to be modified as necessary. The final configuration payload mechanism can be seen in Figure 23.

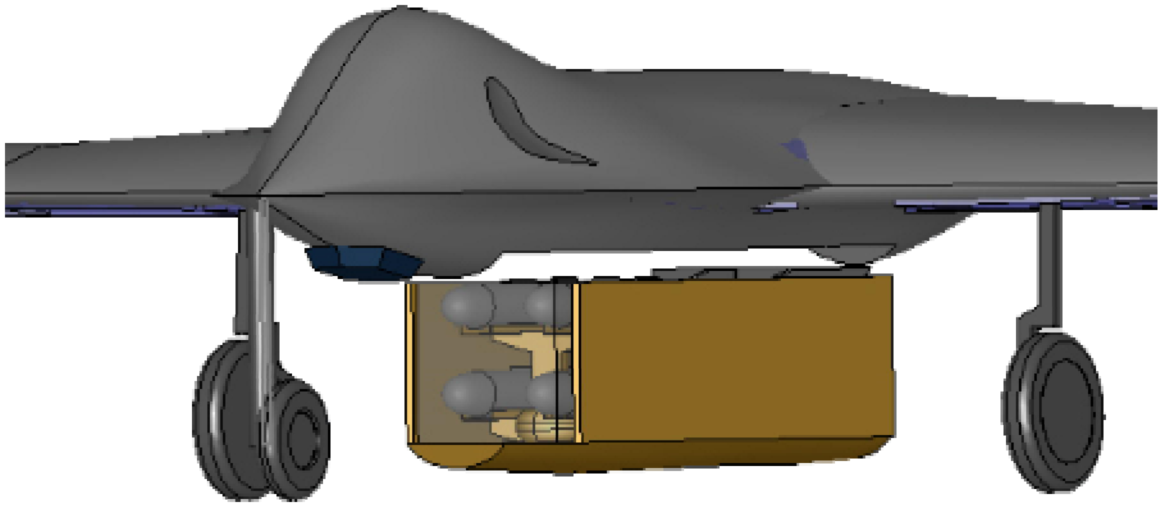

Figure 23- Molniya Palletized Payload System

One foreseeable disadvantage of such a configuration are a possibly higher pitch-down moment that is generated upon extracting the pallet into the airstream – extent of this needs to be investigated, but is unlikely to be of a different magnitude than that created by a other payload deployment means. Finally, the employment of "dumb bombs", although not a part of Molniya's RFP mission might require the development of a standard "hatch" pallet attachment.

4.9. Fuel Tank Configuration

Molniya requires a fuel capacity of 134ft^3 to complete its most fuel-intensive mission. Because of its small overall size, locating the required fuel volume inside the airframe was a challenge. It was decided early on to carry as much fuel as possible within the thick wing of the aircraft. Both the natural thickness of the airfoil and the high volume enclosed by the wing-body joint/strake made *Molniya* able to carry a sizeable fuel load.

Fuel tanks had to be located to make the aircraft controllable during all phases of flight. It was challenging to locate the fuel tanks so that the fully fueled aircraft be stable on takeoff. With the aircraft's center of gravity located near the MAC of the forward-swept wing, no fuel can be located in the rear of the aircraft, where it would create a large pitch-up moment. The fuel tank system implemented in *Molniya* can be seen in figure 24. A set of fuel tanks is located along the span in the thickest part of the chord. With the fuel tank located all the way out to the tips of the wings, the CG does not shift during the mission. Using the active fuel management system implemented in *Molniya*, it becomes possible to move the fuel from tank to tank to keep the aircraft stable throughout the payload deployment maneuver.

Figure 24 - *Molniya* Fuel Tank Configuration

4.10. Controls

The RFP requires that flight characteristics must meet MIL-F-8785B. In order to design *Molniya* for these requirements, initial classification of the aircraft mission, flight characteristics, and quality levels had to be performed. *Molniya*'s design mission classified it as a class IV aircraft, specifically a tactical reconnaissance/attack aircraft.

Although a forward-swept wing does not possess "weathercock stability" in yaw, a control system could easily keep such a configuration stable via drag rudder control. With electronic actuators allowing constant high-frequency responses, the drag losses from the action of the control system should be minimal. The highest concern for a forward-swept-wing aircraft is the possibility of divergent pitch instability. If the aircraft cg is placed in a location not too far back from the aerodynamic chord, a fly-by wire system can deal with the instability present in the aircraft.

Analysis did have to be performed to make sure that the control surfaces had sufficient authority to maintain control of the aircraft. To perform these calculations, a separate program was created in Microsoft Excel. The program was able to interpolate the forces generated on the aircraft at any flight angle of attack, speed and control surface deflection. The program used maps of Cl/Cd/Cm values generated by the XFoil software for the modified TH 25816 airfoil. Using a set of coordinate inputs, moments for the wing, canard-aileron (caileron) and body aerodynamic surfaces were generated. Having the capability offered by this program, a trimmable CG location could be evaluated at various speeds and angles of attack. A typical C_L vs. C_M plot can be seen in figures XX and XX below. The pitch instability of this aircraft configuration is obvious. However, a very important point to notice in the plots below (fig. 25, 26) is that the $C_M = 0$ point is located very close to the loiter CL of 0.65, providing for minimum trim drag at the long-duration loiter condition.

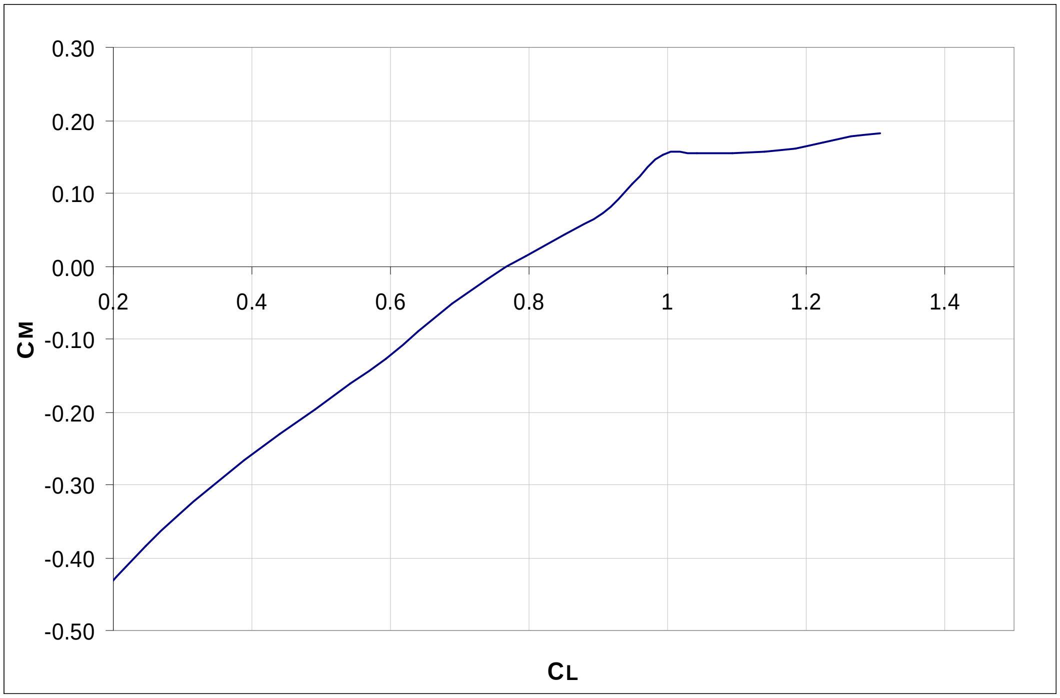

Figure 25 - CM vs. CL @ 0° Caileron Deflection

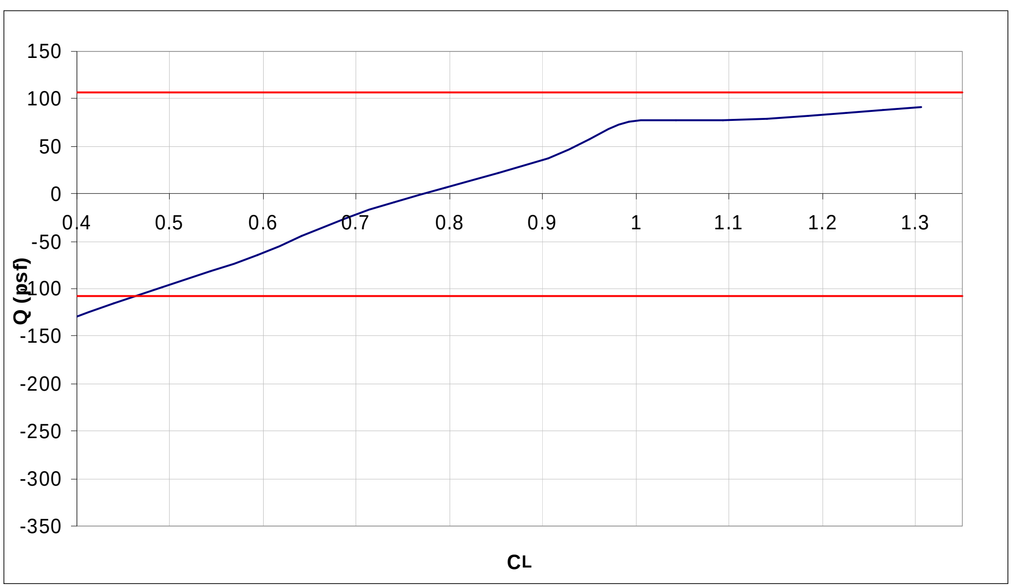

Figure 26 - Q vs. CL @ 0° Caileron Deflection

In order to investigate this aircraft configuration further, a representative aircraft configuration was evaluated using Tornado, a stability and control vortex lattice code. Tornado is a easy-to-use, yet powerful Matlab® add-in software package. Having input a representative configuration into the software, a set of control derivatives could be obtained and evaluated. Pictured in Figures 27 and 28 is the geometry input into Tornado to simulate Molniya's aerodynamic configuration and the software output.

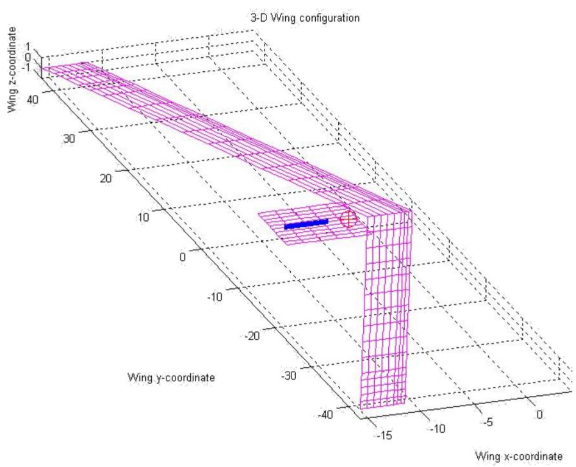

Figure 27 - Sample Geometry Input Into Tornado Software

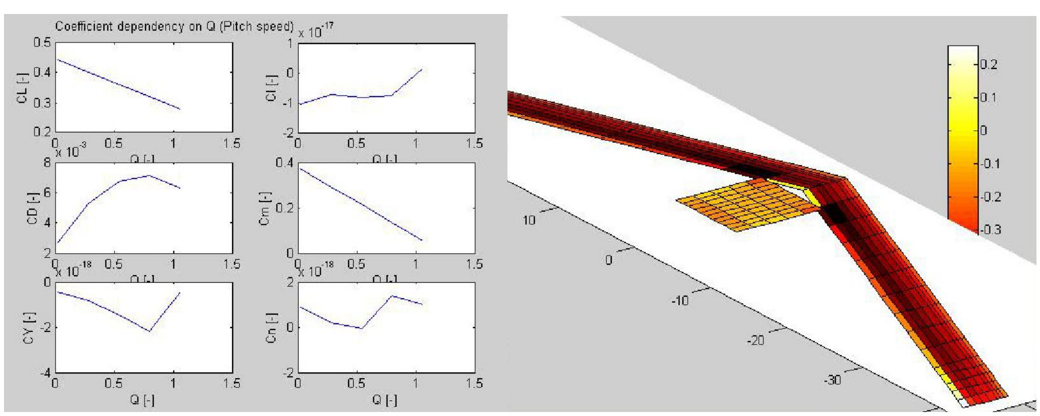

Figure 28 - Tornado Software Output

As a result of performing the evaluation of aircraft geometry in Tornado, a set of control derivatives was created. These control derivatives were derived for a α=0 condition loitering flight and can be seen in table V.

Table V - Tornado Control Derivatives Produced by Central Difference Method

Lift Coefficient		**Drag Coefficient**		**Yaw Coefficient**	
CL-alfa	6.1757	CD-alfa	0.052	CY-alfa	0
CL-beta	0	CD-beta	0	CY-beta	0
CL-P	0	CD-P	0	CY-P	0.052
CL-Q	-12.01	CD-Q	0.960	CY-Q	0
CL-R	0	CD-R	0	CY-R	0.002
Rolling Moment		**Pitching Moment**		**Yawing Moment**	
Cl-alfa	0	Cm-alfa	6.403	Cn-alfa	0
Cl-beta	-0.036	Cm-beta	0	Cn-beta	0
Cl-P	-0.729	Cm-P	0	Cn-P	-0.045
Cl-Q	0	Cm-Q	-23.188	Cn-Q	0
Cl-R	0.128	Cm-R	0	Cn-R	-0.002

The Tornado software confirms the divergent general pitch characteristics derived using the Excel static stability software. Although producing useful results, the software program used a NACA4412 airfoil instead of the TH 25816 airfoil. A surface more representative of the fuselage pod could not be generated in Tornado. Because of this, the pitching moment results of the software can be considered less than reliable. The resulting coefficient in other axis of motion do not show any large deviations. Of interest is the CL-alfa output by the vortex lattice code, a value really close to the ideal 2π, giving more proof to the to the efficiency of the forward-swept wing. Detailed evaluation of the effects of the control derivatives on the aircraft flight characteristics must be performed. A wind tunnel evaluation could likely provide more precise data. However, it seems that the data gathered gives enough support to stating that the current configuration will have stability characteristics that are well within the capability of modern fly-by-wire systems.

5.0 – SYSTEM OPERATIONS

5.1.1 – Vehicle Control

Establishing the mission control requirements for the aircraft required keeping in mind the duality of the RFP mission. The quick reaction-strike mission of the RFP was unlikely be performed by an aircraft operating autonomously. Detecting, prioritizing and firing upon a ground target is not a task that can yet be entrusted to an automated system, both because of technological and ethical issues. The long-endurance data-gathering/light strike mission can certainly benefit from an increase in system autonomy – enabling operators to function more as mission controllers rather than flight crew, only taking over control for the strike portion of flight. However, the Concept of Operations which seems to best fit the mission specified in the RFP still requires constant control over the aircraft by human operators.

Using the above considerations, the UAV mission control level requirement was defined to be level 5 using TCS level definitions.[9] A requirement of the RFP is a Ku-band (12-18Ghz) dish antenna. The 2-ft diameter of the antenna specified allows the aircraft to maintain a duplex data link with the ground station, with the high frequency link providing the aircraft with plenty of bandwidth to send back sensor data in real-time.

Every UAV had a set of distinct mission segments which may require different Command and Control (C^2) technologies. The design mission of *Molniya* requires the following control capabilities:

- Launch and Recovery – A short-range line-of-sight control which guides the aircraft during the takeoff and landing sequences. The LRE (Launch and Recovery Element) facilities are located at the launch site.

- Cruise to/from target – This task is controlled by MCE (Mission Control Element) via the Satcom Ku-band link.
- Loiter– this is the primary mission of the MCE. A pilot and sensor operators control the aircraft and its sensors while loitering over the target.
- Combat – Judging from the RFP requirements, the combat will not occur within visual range of the LRE facilities and will have to be controlled by the mission control segment of the system. With the high bandwidth available via the Ku-band Satcom link, *Molniya* will be able to provide MCE with the information necessary to make a decision to attack.

A schematic of the communications scheme of the operations of the Predator system can be seen in Figure 29. With the high similarity of the two missions, the operational scheme of the *Molniya* will be extremely similar to that of the *Predator*.

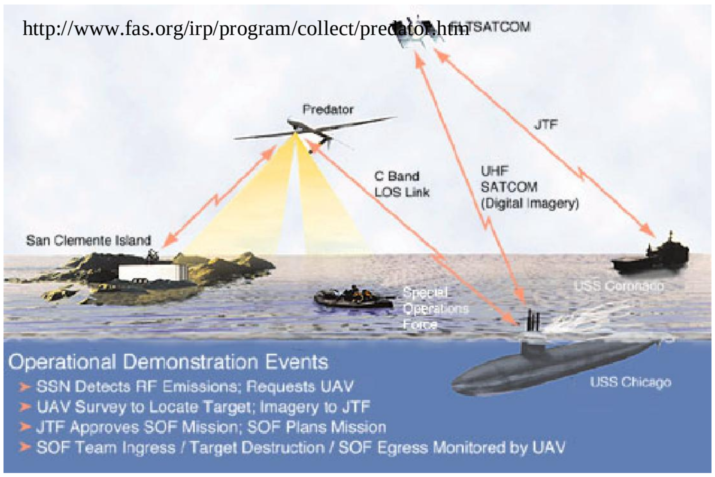

Figure 29 - *Predator* System Operational Schematic

The primary difference between the LRE and MCE is the lack of any wideband data links or image processing capability within the LRE and the addition of a Differential Global Positioning System (DGPS) system at the LRE to provide the precision navigation required for ground operations, take-off, and landing.[10]

To satisfy the control capabilities outlined previously, the aircraft needs to have multiple antennas. An omni-directional LOS antenna is required for the launch/recovery segment of flight. A directional link may be required for long-range line-of-sight communication, such as that encountered in climbing to cruise altitude or above weather which may be affecting Ku-band Satcom operations. Finally, a long-distance over-the-horizon Satcom antenna is required for control during cruise and loiter.

The delay present in the control execution is highly dependent on the communications technology used. Although during the loiter segment, the overall system lag requirement of the *Molniya* is <100 msec, there seems to not be any way to decrease the latency specifically for the combat segment where the requirement is the more constraining <40msec.[11] As such, the acceptable overall system lag is assumed to be <40msec for the long-distance control of *Molniya*. Since the communications are conducted through LEO Satcom and/or Line-or-Sight systems, the system response time is high enough to not be of concern.

5.2 – System Deployment Considerations

Having considered the location of fuel in the airframe and the overall size of the aircraft, it was decided that it would not be advantageous to make *Molniya* able to deploy via cargo aircraft. Instead, in similarity to the *Global Hawk* platform and using the high range of the configuration *Molniya* can self-deploy most anywhere in the world. With *Molniya* being a self-deployable aircraft, a capability to operate in civilian airspace is a requirement. To enable the naturally stealthy aircraft to be tracked while flying through controlled airspace, a set of RF transponders have to be installed or exposed, and communication with air traffic controllers has to be performed. Although current FAA rules do not allow UAVs and manned aircraft to freely share space and fly in the same corridors, changes are likely to occur soon. The aircraft will be designed from the outset to be able to easily operate within the IFR flight environment in order to reduce costs required in future upgrades.

Because of its extremely high range, Molniya is easily deployable. In the example in figure 30 below, a Molniya system is shown to be able to self-deploy to any location in the world from just two bases: USA mainland and NSF Diego Garcia.

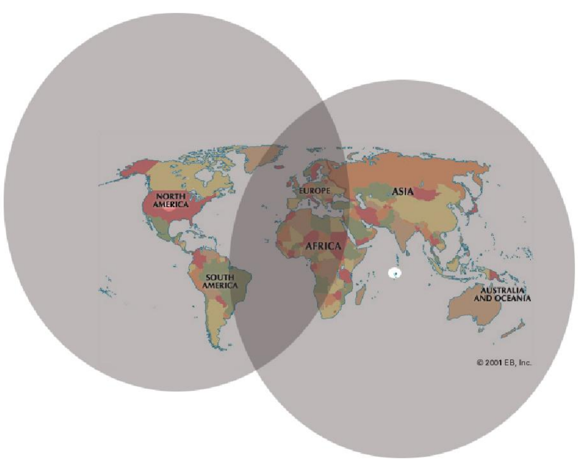

Figure 30– 7500+ Nmi Deployment Radius

Ground station mobility is an issue that affects the mobility of the entire system. Using the standard GCS of the *Global Hawk* system, *Molniya* can be controlled throughout its mission profile. Although with its 7500 Nmi range *Molniya* self-deploys to any part of the world, the L&R section of the system must be moved to the launch site by cargo aircraft.

The current UAV Ground Control Station (GCS) system used to control the *Global Hawk* system is a 30x8x8 foot, triple-axle, commercially available trailer. This trailer is not configured for air mobility and requires special handling to load and unload from C-130 and C-141 aircraft.[12]

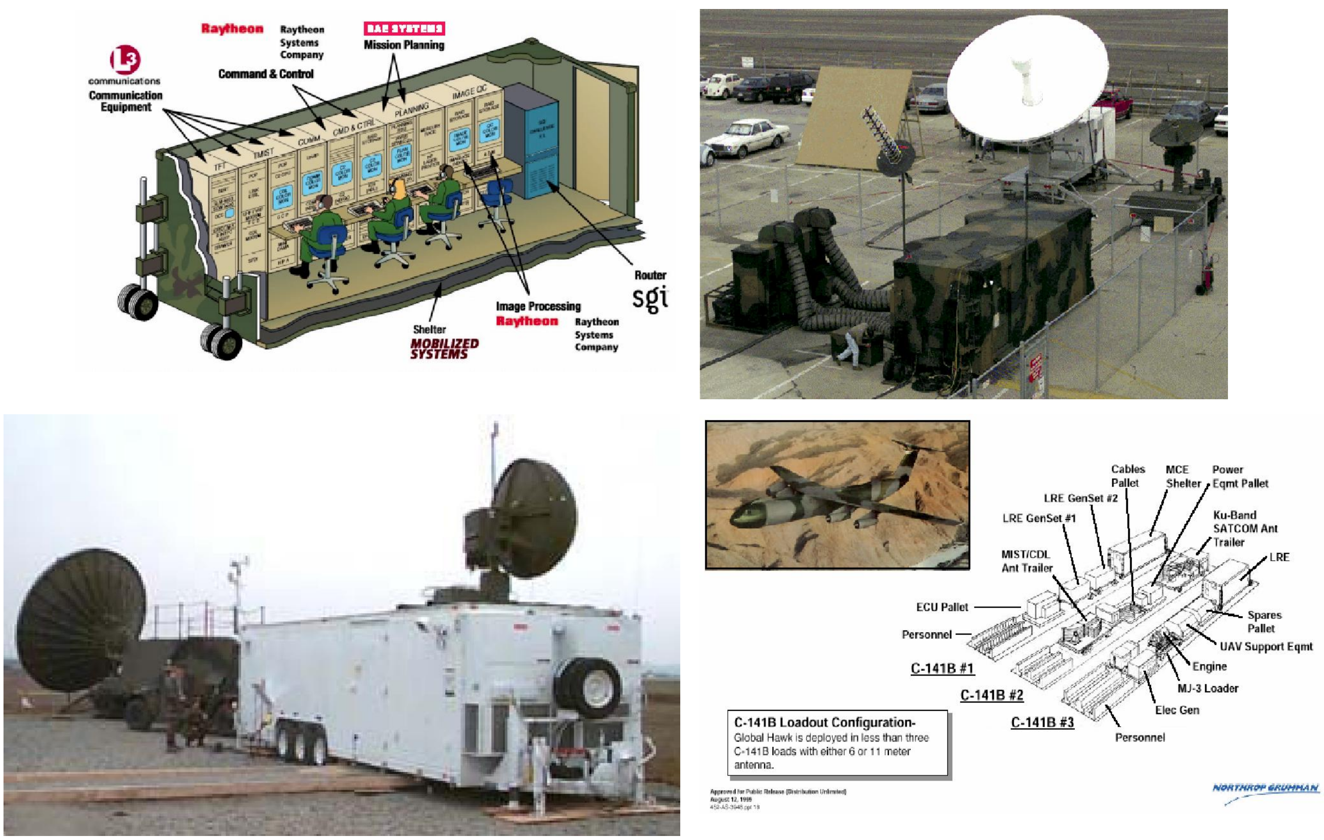

Figure 31 – *Predator* and *Global Hawk* System Ground Control Stations

The above picture shows an example of the deployment of the *Global Hawk* system's MCE and LRE via the C-141B transport.

Although current level of mobility of the GCS segment is presented some concern, it was decided to use the existing GCS of the *Global Hawk/Predator* systems in order to decrease the development costs of the *Molniya* system. As the two systems mentioned above, the *Molniya* UCAV will be designed to incorporate both "return home upon lost link" and self-destruct capability, neither of which should present a significant level of technical difficulty.

5.3 – Survivability

When comparing the mishaps data for manned aircraft and for the predator system, a large disparity can be observed. Compared to manned fighter aircraft with a 4.5 mishaps per 100,000 flight hours, the *Predator* system suffers 27 mishaps in the same time.[13] Some of the main reasons behind UAV losses are many, ranging from poor pilot procedures, aircraft systems testing failures, and in case of the Predator, weather conditions. Because UAVs don't carry a human pilot, they are often designed with a lower level of redundancy, which is likely to contribute to the high accident rates. When considering a system as expensive as Molniya, a higher systems redundancy seems to be a worthwhile investment.

With weather being a leading cause of *Predator* system failures, a high level of importance was placed on incorporating weather ruggedness into the aircraft system. Since *Molniya* is an unstable aircraft, the delivery of accurate flight data to the flight control computer is of crucial importance. In order to prevent icing-over of the pitot tube and to also prevent it from reflecting enemy radar, the pitot tube should be located either in or near the engine intakes or on the upper surface of the aircraft. Anti-icing systems are installed at the crucial locations such as wing leading edges, intakes and at the pitot tube/static pressure ports.

The twin-engine configuration of the aircraft contribute to making it more survivable. As proved by the operational accounts of the A-10 and Su-25 aircraft, the wide separation of the engines decreases the chance of a single hit disrupting the operation of both of the aircraft's engines.

Besides making for a lighter, simpler aircraft, an all-electric controls actuation setup is certain to help to increase the survivability of the system. With modern electric actuators providing higher reliability and response speed than hydraulic systems, making the choice was not difficult. Finally, the integrated multi-directional infrared camera system provides missile launch warning to the aircraft, enabling evasive maneuvers or chaff/flare deployment.

5.4 – Maintenance and Operations

One of the known downsides of the *Predator* system is the relatively high level of maintenance expenses involved with it. It can be theorized that the reason for this downfall is the fact that the vehicle was developed from Leading Systems *Amber* – an advanced technology demonstrator, the development process of which had low emphasis on reducing maintenance cost. In contrast, the *Global Hawk* system was designed to be easily maintainable from the outset of the program and as a result has maintenance requirements that are comparable to those of manned commercial aircraft. Reducing the level of maintenance requirements of *Molniya* to such a degree is highly desirable in a day-to-day operations scenario.

Some of the support/maintenance functions that an aircraft design must be concerned with include, but are not limited to: Maintenance of the engines, airframe and avionics, installation and replacement of weapons and fuel. During the design of *Molniya*, all these issues were taken under consideration and resulted in the following features of the aircraft configuration.

Servicing an aircraft in the field requires a wide variety of access hatches. An important component of affordable stealth technology lies in ensuring that the aircraft components can be serviced without having to restore RAM that covers access hatches. Access hatches that don't require replacing RAM reduces maintenance effort and time on the aircraft and have been implemented on modern stealth aircraft such as the F-22 *Raptor* and the F-35.

Simple engine accessibility through covers in the upper fuselage will be implemented in the production version of Molniya to ensure simple access to these important components. A payload system which allows for easy weapons replacement by the aircraft service personnel is also an important consideration. Aircraft such as the X-45 do not excel in this regard, requiring support personnel to crawl underneath the aircraft to install weapons. The picture below is somewhat interesting, because it shows the X-45 weapons installation scheme, with the ejectors mounted on the weapons prior to installation into the aircraft.

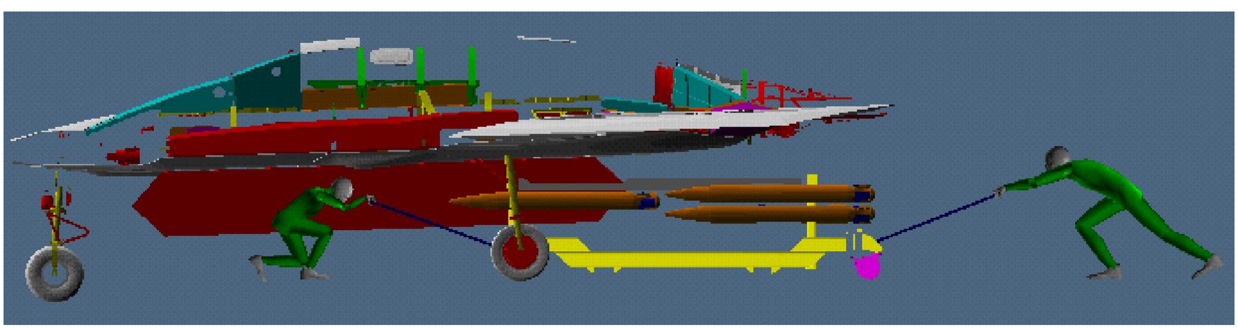

Figure 32 – X-45 Weapons Installation Process.[14]

Weapons loading was expected to be problematic in Molniya's design, since the does not provide much clearance from ground to the bottom of the fuselage. An innovative approach to the payload system was implemented on the *Molniya*.

The operational advantages of such a system are many. First and foremost, the palletized payload system allows for easy and quick weapons installation. After a pallet has been located underneath the UCAV by a standardized weapons loader, it can be lifted into the aircraft, where it engages the retraction system mechanism. Although this mechanism has not been designed in detail, it is unlikely it will cause significant technical problems.

With a palletized weapons system, an aircraft configuration can be made more flexible – a *Molniya* system could have multiple pallets outfitted for different weapons payloads all ready for immediate installation. Special pallet materials could be used for sensor missions that require a “see-through” aircraft surface. Finally, this enables a simple attachment of a fuel tank to the aircraft if required for extra-long deployment range.

5.5 – Systems Cost

The systems acquisition costs were scaled using a CPI index[15] of 0.906 to adjust prices from ’99 to ’03.

An advanced technology cost factor was added to the price of airframe components, to accurately reflect the respective decrease in empty weight that this produced. An assumption in the cost calculations was made which stated that Electro Optical Sensor packages be constructed for only ½ of the airframes. A similar assumption was made when setting the number of GCS as ¼ of the number of airframes. The cost for the GCS was the quoted cost of the Predator System GCS, which was also described as being employed in the 1 GCS per 4 AV ratio.

Table VI – Systems Costs Calculation Inputs

Maximum Velocity	347.27	kts					
Empty Weight	5204.3	lbs			Mult	Tot (K$)	Tot (M$)
Number of test aircraft	4		NRE (khrs)	1081	86	92997	$93.00
Structure			NRT (khrs)	566	88	49792	$49.79
Production Quantity	100		DS (K$)	24814			$24.81
Turbine Inlet Temp	2250	deg R	FT (K$)	16399			$19.28
			RE100 (khrs)	400	86	34369.42	$34.37
NRE - Non Recurring Engineering Hours			RT100 (khrs)	388	88	34158.01	$40.16
NRT - Non Recurring Tooling Hours			RML100 (khrs)	2669	73	194825	$229.06
DS - Development Support Cost			RMM100 ($)	54066			$63.57
FT - Flight Test Cost			RQA100nc (khrs)	355	81	28751.37	$28.75
RE100 - Recurring Engineering Hours			Raymer Engine	317841	100	31784.12	$31.78
RT100 - Recurring Tooling Hours			Avionics	785	5000	392500	$392.50
RML100 - Recurring Manufact. Labor Hours			EO Payload	600	5000	300000	$150.00
RMM - Recurring Manufact. Material Cost							
RQA - Recurring Quality Assurance Hours							

Table VII - Programme Costs Calculation

Vehicle		
	Nonrecurring	$2.1Million Dollars
	Recurring Total	$10.7Million Dollars
	Total Cost	$12.8Million Dollars
GCS		
	Total Cost	$1.4Million Dollars
Package		
	Total Cost	$14.2Million Dollars
Programme		
	Nonrecurring	$206.27MD
	Recurring Total	$1,208.82MD
	Total Cost	**$1,415.09MD**

It can be seen that the price of the Molniya unit airframe and programme are both below that required by the RFP.

5.6 – Life Cycle Costs[16]

In order to determine operational costs of the *Molniya* system, a set of variables needs to be known. The minimum information required is: Number of personnel, flight hours per year, cost per flight hour, other direct cost and indirect personnel. The *Predator* system uses 13.75 persons per air vehicle, 4 of whom are aircraft maintainers. Because one of the main goals of the Molniya system is a dramatic decrease in maintenance personnel required, a decrease in maintenance requirement to that of the Global Hawk system can be expected.

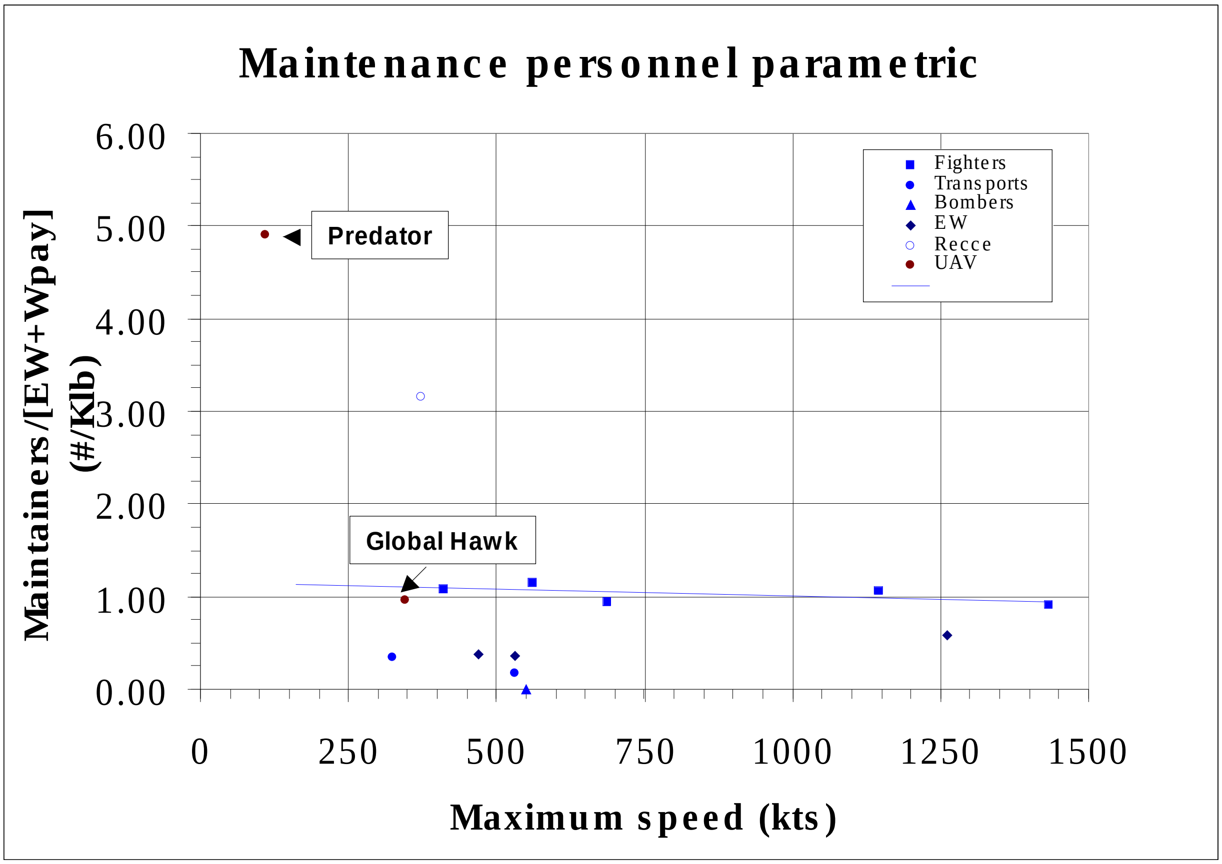

Figure 33 - Maintenance Personnel Requirements[17]

Using the trend line in figure 33, a value of 1.2 of Maintainers/[EW+Wpay]*(1/1000) can be derived. This gives a value of 6.9 maintainers per air vehicle for the *Molniya* system. Next, an assumption of 25% is made for an indirect personnel cost ratio in order to account for the costs related with security, medical and other expenses. Assuming a personnel cost of $51.5K 2003 dollars per maintainer per year, the total personnel + indirect cost will be $444K per year per *Molniya* system.

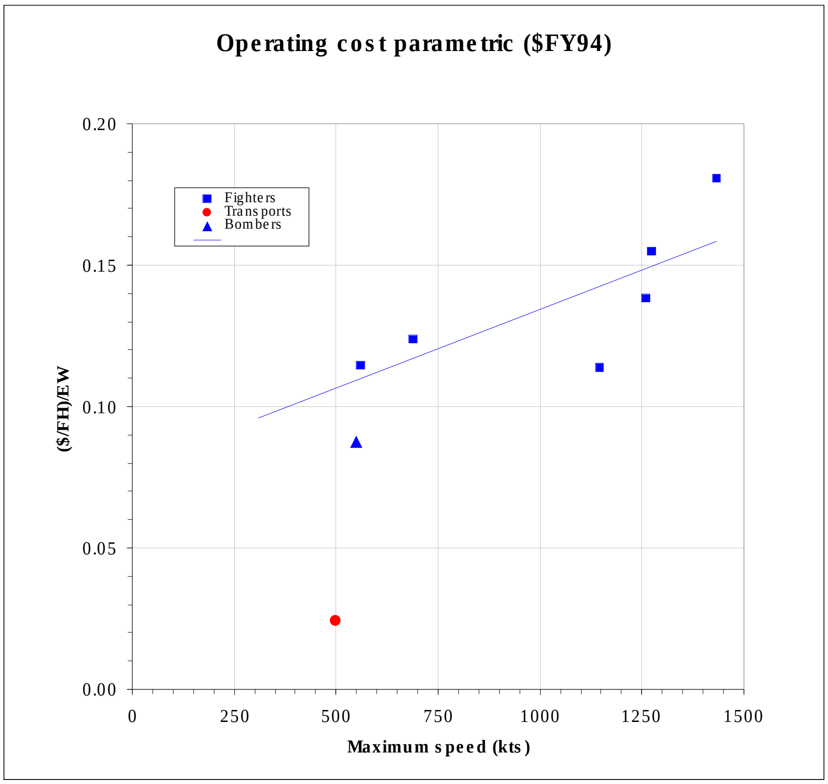

Figure 34 - Operating Cost vs. Maximum Speed[18]

The cost per flight hour can be derived from Figure 34, using the maximum speed of 350kts as. At 1000 flight hours per year at $0.1,0 ($/flt_hr)/EW_lb, the air vehicle operating costs would be $700K/year in FY94 dollars. Scaling this to FY2003 using a CPI index of 0.806, we get an operating cost of $868,5K/year. Both payload and ground station/comms operations and support costs (O&S) can be assumed at 8% procurement cost per year. Using this assumption, a value of $44K/year was calculated for the EO package and $100K/year for the GCS. Once again, the EO package costs were split between 2 *Molniya* airframes, and the GCS costs between 4. The above calculation gives a final operating cost of **$1.28M** per *Molniya* air vehicle per year. Compared to the quoted O&S price[19] of $1.81M per *Predator* air vehicle per year, the Molniya system provides not only a dramatic increase in performance but also a great decrease in operational cost.

6.0 – PERFORMANCE

An RFP requirement that caused high concern was the 1-g specific excess power requirement, which the RFP specified as 100ft/sec at 25,000ft and Mach 0.5. Designing an aircraft to adhere to this requirement would oversize the installed power of the configuration, causing extremely high SFCs at loiter and a tremendous gross weight increase. For example, the current configuration requires roughly 9 times the thrust installed on the aircraft to obtain such performance. Considering the loiter/light attack mission profile of *Molniya*, the performance level stated in the above requirement seemed to be extremely arbitrary. It was assumed that this requirement was a result of an error and a decision to take an exception on this aspect of the RFP was made.

With the above mention, the 1-g military 100% thrust specific excess power envelope can be seen in Figure 35 below.

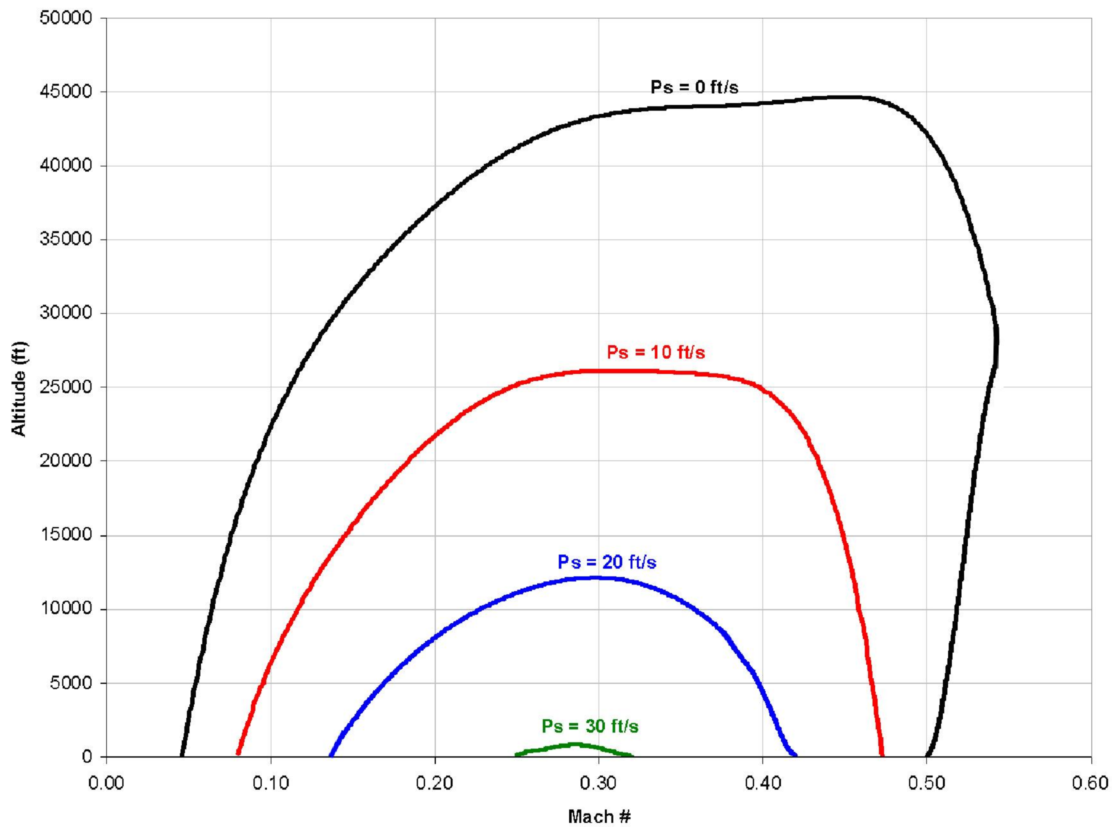

Figure 35 - 1-g Maximum Thrust Specific Excess Power Envelope

The figure shows that the maximum excess power that *Molniya* can attain at the loiter altitude of 25k ft. is very close to 10 ft/sec. This condition occurs at a maximum Mach number of 0.4, which is equal to 406 ft/sec at that altitude. A set of similar performance trends can be seen in the 2-g specific excess power envelope presented in Figure 36 below.

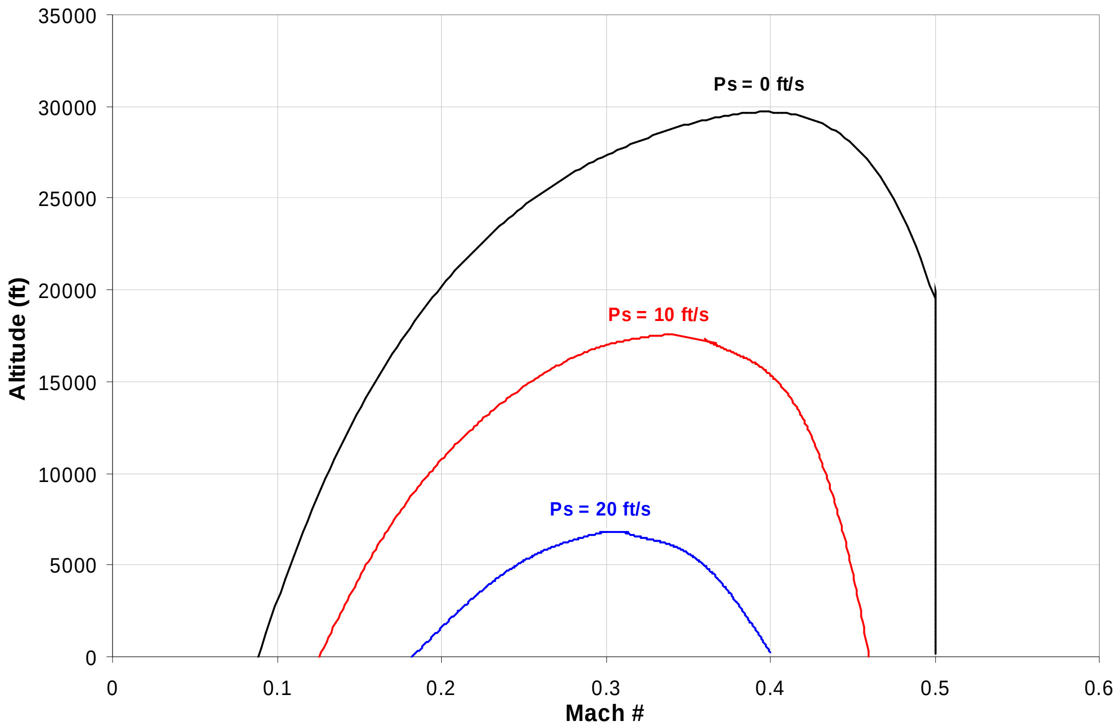

Figure 36 – 2-g Maximum Thrust Sustained Load Factor Envelope

The Maximum Thrust Maneuvering Performance plot and the 5-g Maximum Thrust Specific Excess Power Envelope plot can both be seen in Figure 37 below. From the figure it can be seen that *Molniya*, not designed as an extremely maneuverable vehicle does not possess the thrust required to maintain a 5-g maneuver at most of its flight envelope.

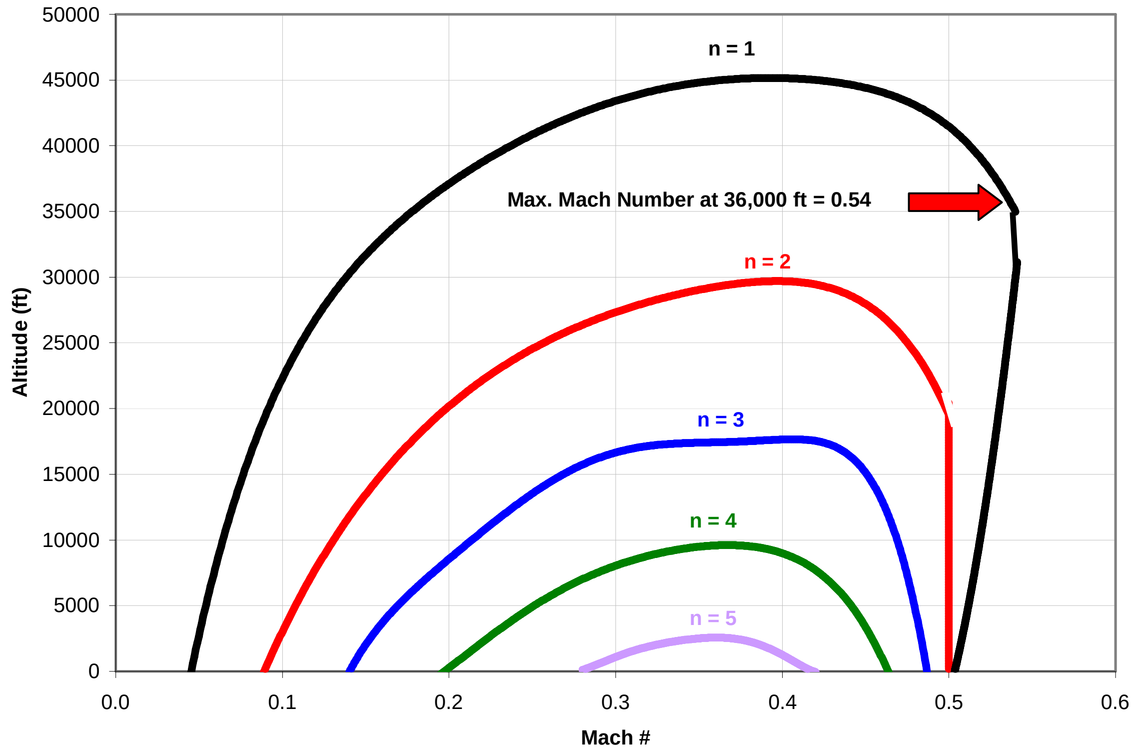

Figure 37 - Maximum Thrust Maneuvering Performance

Molniya performs the all of the missions required by the RFP. Following are the mission fuel burn statistics, listed by mission segment in Table VIII.

Table VIII - Mission Fuel Burn

	Surveilance/Light Attack	**Quick Reaction Strike**
Gross Takeoff Weight	**12500 lbs**	**6950 lbs**
Climb	12500 – 12400 lbs	6950 – 6925 lbs
To Target	12400 – 12300 lbs	6925 – 6880 lbs
Loiter	12300 – 6660 lbs	N/A

Combat	6660 – 6650 lbs	6880 – 6870
Assess	6650 – 6110 lbs	6870 – 6220 lbs
From Target	6110 – 6050	6220 – 6030 lbs

The fuel consumption values listed for the Surveillance/Light Attack mission above are for the non-combat/surveillance-only version of the mission. The 600 lb payload is assumed to be retained within the aircraft and brought back to base, making this the most fuel-intensive mission specified by the RFP.

The time spent during each of the mission segments can be seen in Table IX.

Table IX – Mission Time Breakdown

	Surveilance/Light Attack	**Quick Reaction Strike**
Takeoff and Climb	15 min.	3 min.
To Target	22 min.	12 min.
Loiter	30 hr.	N/A
Combat	2 min.	2 min.
Assess	5 hrs.	5 hrs.
From Target	31 min.	12 min.
Reserve	15 min.	15 min.

When performing the Quick Reaction Strike Mission, *Molniya* does not need to carry its full load of fuel. Because of this lower loading, the aircraft can perform the mission while flying with a gross weight some 5500 lbs lighter than during the loiter/light attack mission. By flying with such a low weight, the thrust required during the Mach 0.6 dash is reduced dramatically. In sizing of the aircraft, the thrust installed and the wing area of the configuration were optimized – as a result, the configuration uses almost 100% of the thrust available during both of the configuration drivers - the takeoff and the dash segments.

It should be noted that when executing the quick reaction strike mission, the *Molniya* dashes back at Mach 0.6. This burns slightly more fuel than a cruise at optimum speed would, however is done intentionally. It can be assumed that in a situation which demands the quick-strike mission, the turn-around time to bring more payload to “the hotspot” is likely to be at a premium. If the return leg of the mission were to be flown at optimum speed, the amount of fuel consumed would decrease from 192 lbs to 50 lbs, but the flight would take more than 10 minutes longer.

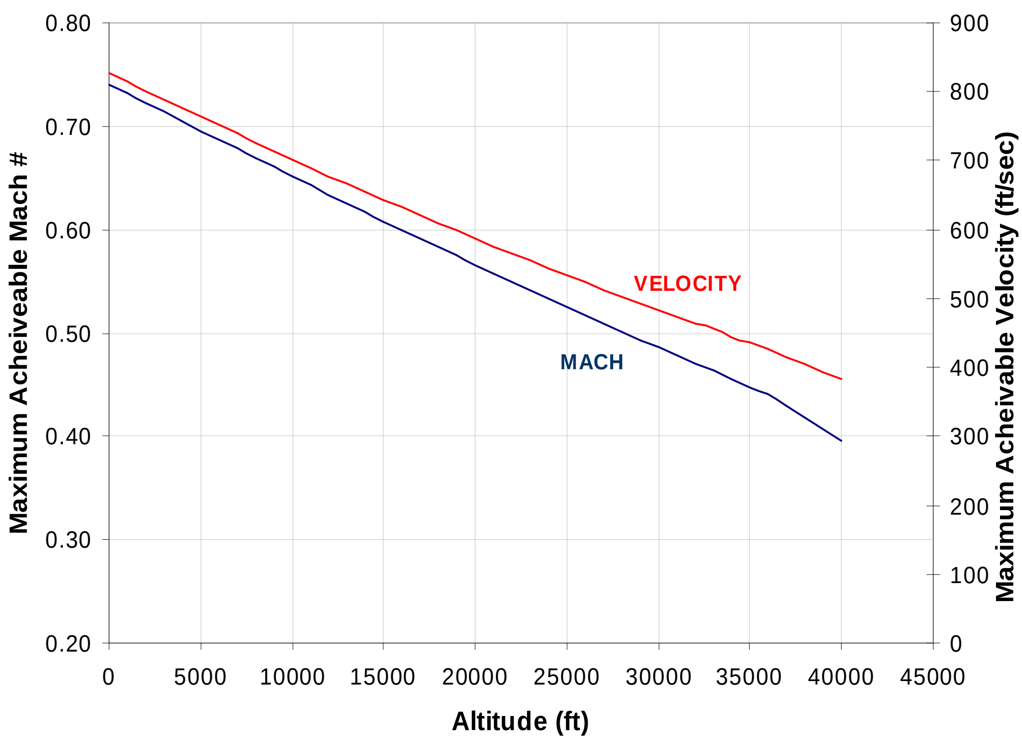

Figure 38 - Max. Mach Number and Velocity vs. Altitude

The critical case for the takeoff accelerate-brake constraint is the icy runway with its low coefficient of friction. Because mechanical braking is practically useless, and aerodynamic braking is not very efficient at the low speeds *Molniya* takes off at, a method to rapidly stop the aircraft had to be implemented.

The simplest and least risky approach was the traditional thrust reverser installation. When activated, the thrust reverser opens a hatch on the top surface of the aircraft, rerouting the exhaust gases forward. It was assumed that during operation, the thrust reverser would be 45% effective in reversing the maximum engine thrust.

With the accelerate-brake distance being a strong driver for high installed thrust, the standard takeoff sequence was not difficult to perform. The aircraft needs a climb slope of only 1° in order to clear the 50 ft. obstacle at the end of the runway. This is equivalent to a climb rate of roughly 4ft/sec, which *Molniya* can be seen to easily obtain at takeoff speed, sea level. Molniya's profile on takeoff can be seen in Figure 39.

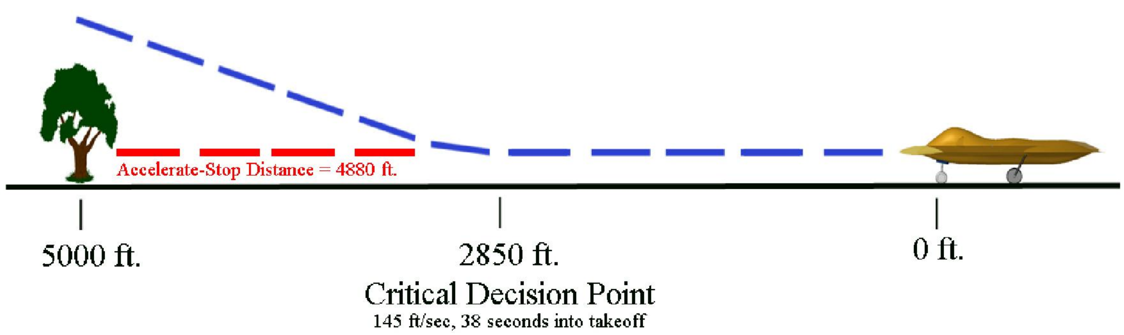

Figure 39 – Aircraft Takeoff Performance

7.0 – CONCLUSION

The Gisin Aviation *Molniya* system has been demonstrated as the optimum solution to the AIAA 2002/2003 Individual Aircraft Design RFP. Because of the multi-directional design approach undertaken, the Molniya system was developed in an extremely short period of time to excel in the RFP mission. Although incorporating various innovations and obtaining performance gains from an untraditional airframe configuration, the aircraft is otherwise quite conventional and rugged in its daily operations scenario. With its superior performance, it is the perfect replacement for the vulnerable *Predator* system and will be able to be on service to the United States military for many years into the future.

APPENDIX A – ENGINE DECK – PROJECTED AGILIS TF1000

Mach #	Thrust (lbf)	% Max	Appox. SFC	FJ44 SFC
0.1	1700	1.00	0.48	0.538
0.1	1600	0.94	0.48	0.5375
0.1	1400	0.82	0.47	0.5252
0.1	1200	0.71	0.47	0.5251
0.1	1000	0.59	0.47	0.525
0.2	**1510**	**1.00**	0.54	**0.6**
0.2	**1400**	**0.93**	0.53	**0.59**
0.2	**1200**	**0.79**	0.52	**0.575**
0.2	**1000**	**0.66**	0.51	**0.57**
0.3	**1370**	**1.00**	0.59	**0.659**
0.3	**1200**	**0.88**	0.57	**0.6375**
0.3	**1000**	**0.73**	0.56	**0.622**
0.3	**800**	**0.58**	0.55	**0.6125**
0.3	**600**	**0.44**	0.55	**0.608**
0.3	**500**	**0.36**	0.55	**0.607**
0.4	1250	1.00	0.65	0.725
0.4	1200	0.96	0.64	0.715
0.4	1000	0.80	0.61	0.677
0.4	800	0.64	0.60	0.6625
0.4	600	0.48	0.59	0.65
0.4	400	0.32	0.60	0.6625
0.4	300	0.24	0.61	0.675
0.5	1125	1.00	0.72	0.8
0.5	1000	0.89	0.69	0.7625
0.5	800	0.71	0.65	0.72
0.5	600	0.53	0.63	0.7
0.5	400	0.36	0.63	0.7
0.5	300	0.27	0.64	0.7125
0.6	**1000**	**1.00**	0.81	0.9
0.6	800	0.80	0.71	0.78333
0.6	600	0.60	0.67	0.745
0.6	400	0.40	0.66	0.73333
0.6	300	0.30	0.68	0.755

References:

[1] http://www.ae.utexas.edu/ASE261KChaput/Lesson12.ppt

[2] Raymer, D. P. Aircraft Design: A conceptual Approach – Third Edition, AIAA, Washington DC, 1999

[3] http://www.awgnet.com/shownews/00nbaa2/hardwr10.htm

[4] http://www.rand.org/publications/MR/MR1596/MR1596.pdf

[5] http://www.djaerotech.com/dj_askjd/dj_questions/forwardswept.html

[6] http://www.stk.com/products/explore/partner_products/radbase_prod_desc.htm

[7] http://www.fas.org/irp/imint/niirs.htm

[8] http://uav.navair.navy.mil/database/matrix.htm

[9] http://www.fas.org/irp/program/collect/uav_tcs.htm

[10] http://www.fas.org/irp/doddir/usaf/conops_uav/part02.htm

[11] http://www.ae.utexas.edu/ASE261Kchaput/Lesson9.ppt

[12] http://www.fas.org/irp/program/collect/uav_gcs.htm

[13] *Class A Cumulative Mishap Rate, 1997

[14] http://www.ae.utexas.edu/ASE261KChaput/lesson11.ppt

[15] http://oregonstate.edu/Dept/pol_sci/fac/sahr/cv2003.xls

[16] http://www.ae.utexas.edu/ASE261KChaput/lesson13.ppt

[17] http://www.ae.utexas.edu/ASE261KChaput/lesson12.ppt

[18] http://www.ae.utexas.edu/ASE261KChaput/lesson13.ppt

[19] http://www.ae.utexas.edu/ASE261KChaput/lesson13.ppt